SPACE · POWER · AND PROPULSION SECTION

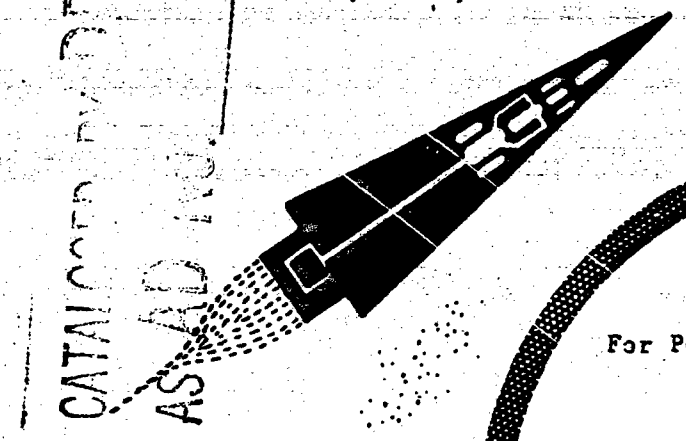

QUARTERLY REPORT #5

For Period Ending July 15, 1963

DYNAMIC SHAFT SEALS IN SPACE

Under Contract #AF33(637)8469

For

Aeronautical Systems Division
Wright Patterson Air Force Base, Ohio

MISSILE and SPACE DIVISION

GENERAL ELECTRIC

CINCINNATI, OHIO

SPACE POWER AND PROPULSION SECTION

QUARTERLY REPORT NO. 5

JULY 15, 1963

DYNAMIC SHAFT SEALS IN SPACE

Under Contract #AF 33(657)-8469

RE-ENTRY SYSTEMS DEPARTMENT
MISSILE AND SPACE DIVISION
GENERAL ELECTRIC COMPANY
CINCINNATI 15, OHIO

TABLE OF CONTENTS.

LIST OF FIGURES

I. SUMMARY

The Space Power and Propulsion Section of the General Electric Company has been under contract to the Aeronautical Systems Division, Wright Patterson Air Force Base, Ohio, since April 15, 1962, for the development of dynamic shaft seals for space applications. The objective of this program is to acquire the techniques for sealing high speed rotating shafts under the operation conditions of high temperature liquid metals and vapors, the near-vacuum environments of space, and to provide long seal life.

A. The contract specifies the following requirements:

1. The fluid to be sealed shall be potassium.
2. The seals shall be operative at fluid temperatures from the melting point of the fluid selected to 1400°F.
3. The pressure on the fluid side of the seal shall be 15 psi and the external pressure shall be 10^{-6} mm Hg.
4. The speed of the rotating shaft shall be a maximum of 36,000 rpm.
5. The seal, or seal combinations, shall be designed for 10,000 hours of maintenance-free life.
6. The working fluid, potassium, shall be used as the seal lubricant.
7. The seal, or seal combinations, shall be capable of maintaining zero leakage - in the technical sense - under all conditions of operation.
8. The seals shall be designed for a 1.0 inch diameter shaft.
9. The seals shall be capable of operating in a zero "g" environment.

B. The seal evaluation shall consist of:

1. Preliminary experiments with water.

2. 100-Hour operational screening test with liquid metal.

3. Thermal-cycling test with liquid metal.

4. 3000-Hour life test with liquid-metal.

This report covers progress during the quarter ending July 15, 1963. The main events of this reporting period are:

1. The interface instability observed during the operation of dynamic fluid ring seals continued to be investigated. Several methods of suppressing the instability leakage using waster as the seal fluid have been developed. These methods are not dependent on close axial clearances.

2. Metallurgical data on the materials used in the liquid metal test rig have been obtained and the information used to insure proper design of the equipment. Additional data on the welding and heat treatment of the Rex 49 gas bearing shaft material is still being investigated.

3. Analysis of the operating characteristics of the argon gas bearing for the liquid metal test rig has been made with a program on the 7090 computer.

4. Quotations for manufacture of the liquid metal test rig have been received and the lowest bidder selected. The low bidder was then investigated to determine that he was capable of manufacturing tolerances necessary in the gas bearing. The manufacturing order was then placed with a scheduled delivery date of December 31, 1963.

5. The manufacturing order for the liquid metal seal test facility has been placed. The delivery date for the facility is scheduled for November 7, 1963.

The following events are forecast for this coming quarter:

1. Completion of all seal testing utilizing the water seal test rig located in Building 301. This includes optimization of rotating housing/disk seal configuration which will be used in the liquid metal test rig seal design.

2. Technical analysis and presentation of the rotating housing, rotating disk and squeeze seal will be completed. This analysis includes an integration of test data and theory.

3. Manufacture of the liquid metal seal test rig should be completed and ready for delivery to Evendale.

4. Manufacture of the liquid metal seal facility will be completed and installation of the facility in Building 314 will be in progress.

5. Analysis of the argon gas bearing will be completed. This analysis will provide operational data for the test rig.

6. The materials investigation for the liquid metal test rig will be completed and the information used in the test rig manufacture.

VI. FLUID DYNAMIC TESTING

The testing on the rotating disk seal and the squeeze seal was performed during this reporting quarter. This testing was required for the additional investigation of the interface stability phenomena associated with non-contacting rotating seals. For the purpose of this investigation, the double disk seal configuration mounted on the 20,000 rpm test spindle was utilized because of its adaptability to disk and stationary wall changes and the excellent observation capability afforded by the clear plastic stationary wall. The disk configuration also allowed rapid change in the inlet/outlet configurations and the use of more than one outlet.

Interface instability or sputtering phenomena has been observed many times throughout the rotating disk seal testings. The degree of the instability varied with the water ring velocity and the water ring depth. Physically the instability is characterized by the seal fluid breaking through the fluid surface next to the stationary wall and leaking out of the seal cavity from that point. It may be seen that the breaking through of the fluid surface occurs when the tangential velocity of the sealing fluid is of a much lower velocity than the radial flow in the inward direction. It is therefore postulated that the surface penetration of the fluid is caused by radial flow surpluses that cannot be activated in the tangential direction at the stationary wall. This flow field occurs because of the characteristic viscous fluid profile within the seal cross-section. The velocity of the sealing fluid in a tangential direction is greatest on the surface of the moving or driving member of the seal and necessarily zero at the stationary portion or stationary

wall of the seal. The maximum tangential velocity occurring at the moving member is identical to the velocity of the rotating disc.

Methods have been tested which provide complete sealing using water as a working fluid up to speeds of 20,000 rpm utilizing a seal diameter of 3 9/16 in. All methods are dependent on close mechanical clearances and some of the more attractive schemes impose a high parasitic heat load on the seal system. Sealing schemes which involve close axial clearances are the most abundant and most easily manufactured. However, their usefulness is limited to applications near the thrust bearing in turbo-machinery. At a great distance from the thrust bearings the thermal growth of the shaft or the outer casings are of such a magnitude that close axial clearances are impractical and cannot be maintained. Therefore, sealing schemes which involve only close radial clearances seem to be the only practical way of designing non-contacting seals. Sealing schemes of this type are more difficult to design since any such design necessarily increases the overall seal length because of the flow paths that must be devised to eliminate any fluid leakage.

Because of the simplicity of potential seal designs involving close axial clearances many of these designs were investigated on our 20,000 rpm water seal test rig. This hardware for the rotating disk stationary walls studies will now be further discussed in a summary of the observed interface instability.

Photographs of hardware designed and tested for the specific purpose of eliminating leakage from interface instability are shown in Figures 2 and 3 of this report. In addition to these photographs numerous other modifications

have been investigated. Motion pictures were also utilized in this study to provide comparisons between the various configurations designed. The significant contribution of the motion pictures was a recording of test run observations of the seal configurations at 5,000, 10,000 and 15,000 rpm. A summary of the rotating disk configurations will now follow:

1. Plain rotating disk and plain stationary wall.

The plain rotating disk shown in Figure 2 and labeled No. 1 and the stationary wall shown in Figure 3 and labeled No. 5 were originally tested. It was intended from the seal proposal that this configuration would provide a satisfactory seal with a stable liquid to vapor interface. However, since the early testing proved that interface instability was prevalent and resulted in the loss of the seal fluid, it became necessary to proceed beyond this state of the art.

Testing of the plain disk and wall elements revealed that leakage occurred at the stationary wall and any leakage was subsequently lost overboard and not returned to the seal fluid sump. The leakage occurred at random while using these elements. Occasionally, it was possible to prevent leakage to speeds as high as 10,000 rpm, but once the leakage occurred it was impossible to stop the leakage even by decelerating to speeds as low as 1,000 rpm. The problem that presented itself throughout the testing of this configuration was the lack of repeatability of any of the instability results. The leakage occurred at the stationary wall and, since it was postulated that this leakage was caused by an excess of radial flow within the seal cavity, it was desirable to design stationary wall elements that would prevent this radial inflow and, hopefully, the leakage. Therefore, Configuration No. 2 was designed with this requirement.

2. Plain rotating disk and grooved stationary wall

The plain rotating disk shown as No. 1 in Figure 2 and the grooved stationary walls shown as No. 1 in Figure 3 were used for this investigation. It was expected that by introducing various grooves in the stationary wall that the radial inflow could be reduced to an acceptable level and proper sealing established. However, extensive investigation with this configuration revealed repeated seal leakage whenever speeds above 10,000 rpm were encountered. But leakage repeatability at low speeds was not necessarily consistent. The reason for this inconsistency was not determined since it was apparent that this type of seal configuration would be unacceptable for the use in this contract.

3. Plain rotating disk and lip stationary wall

The plain rotating disk and the lip stationary wall shown as No. 3 in Figure 3 was designed to prevent leakage from the seal cavity when an unstable liquid-vapor interface existed. It was intended that the lip on the inside diameter of the stationary wall would return the fluid which escaped from the seal fluid surface. This design proved to be inadequate for extending the operational range of the rotating disk seal. Testing revealed that operation with this configuration was similar to the plain rotating disk and grooved stationary wall.

4. Rotating disk with helix and groove/lip stationary wall

The rotating disk with helix shown as No. 4 in Figure 2, was characterized by the introduction of a positive means of returning the escaping water to the seal cavity. This feature did not exist in any of

the previously tested seal configurations. The helix on the rotating disk surface was used to return the escaping seal fluid. The groove lip portion of thestationary wall was also run with zero axial clearance on the rotating disk. The configuration allowed speeds as high as 15,000 rpm without any significant leakage. Leakage which occurred at speeds of even 20,000 rpm was of only droplet sizes and at an extremely slow rate. However, once the zero clearance between the stationary lip and the rotating disk was opened because of the rubbing contact, leakage was rapidly increased. This leakage then reached a magnitude which was entirely unacceptable and was of the order of magnitude similar to those leakages in Configurations No. 2 and No. 3.

5. V-groove rotating disk and stationary wall combination

The V-groove rotating disk is shown as No. 3 in Figure 2. This seal configuration has previously been used for establishing a vapor liquid interface in rotating machinery. The mechanism of the seal requires that any leakage which might occur along the stationary wall of the seal must necessarily come in contact with the protrusions on the surface of the rotating disk when the design requirement of low axial clearance is maintained.

Investigation with this sealing principle revealed that acceptable sealing was maintained at speeds in excess of 10,000 rpm when axial clearances of .020 were maintained. However, at speeds greater than 13,000 rpm the leakage reliably occurred. It seems possible that if

seal diameters of greater than 3½" were available additional V-grooves could be installed and the onset of leakage extended to even higher speeds. However, this seal configuration encountered high parasitic losses because of the submerged boundary layers of the working fluid on the rotating disk and stationary wall. The submerged boundary layers caused excessive power losses and consequently high heat losses. Also, because of the close clearances being maintained it was impossible to properly circulate the seal fluid and overheating becomes a potential problem.

6. Screw return rotating disk and plain stationary wall

The screw return rotating disk shown in Figure 2 as No. 5 and plain stationary wall were employed to prevent the water leakage associated with the interface instability. The design intent of this configuration was to return any seal fluid that was lost from the seal interface along the stationary wall to the seal cavity by use of screw threads in the annulus between the rotating shaft and stationary wall.

This configuration provided acceptable sealing to speeds above 10,000 rpm with a radial screw clearance of .005 of an inch. However, at speeds greater than 10,000 rpm and less than 15,000 rpm leakage occurred repeatedly and could not be stopped by the screw threads. This performance is synonomous with the sputtering which occurs with the screw seals at high velocity. It should be pointed out that the threads employed in this application had a small helix angle and therefore, provided better sealing performance than would have been accomplished if the coarser thread such as the optimum values reported in the screw

test work in the third quarterly report had been used. The feasibility of using this device at low speeds appeared to be better than any other seal configuration tested to 15,000 rpm. However, it should be understood that complete sealing with this configuration at high speeds was not obtainable.

7. Screw return rotating disk with vanes and plain stationary wall

The screw return rotating disk with vanes was identical to the preceding screw return rotating disk discussed above except that the disk had several vanes within its body to return the fluid from the screw portion near the I.D. of the disk to the outer tip diameter. The usefulness of this disk was of negative value. The configuration No. 6 performed as good or better on every account than did this one.

8. Long paddle rotating disk with V-groove

The long paddle rotating disk with V-groove is shown as No. 2 in Figure 2. This seal configuration provided paddles with which to increase the watering velocity within the seal cavity and provided a groove near the I.D. to limit the possible instability leakage. This configuration was also dependent on close axial clearances and failed to perform as designed whenever the axial clearance for the V-groove increased beyond contacting limits.

Examination of this seal configuration by the use of a strobe light revealed that the water within the seal cavity was filled with foam. The foam within the seal cavity was due to the action of the paddle wheels on the fluid. In addition, theheat losses due to the excessive agitation

of the water within this seal cavity were considerably higher than those experienced with the previously tested configurations. Based on these results, and the results of the sputtering observations, it could be seen that this configuration was not a desirable one from the seal standpoint. Leakage due to the interface instability occurred at speeds of approximately 10,000 rpm. The leakage was similar to those experienced with other configurations. However, this configuration revealed a potential improvement which might possibly provide a useable seal. This improvement consisted of shortening the paddle blades and providing a disk surface and a blade surface near the inner diameter.

9. Short paddle rotating disk with V-groove

The rotating disk used for this configuration had shortened paddles from the configuration tested above. Visual observation with the use of strobe light revealed this configuration to have a much more stable seal surface. However, leakage losses were not improved. The power losses due to the excessive agitation of the working fluid were significantly reduced from the long paddle configuration.

10. Rotating disk/housing seal

This seal was designed near the end of the reporting period and consequently, is not shown in photograph form. However, the seal depends on close radial clearances for its operation and sealing has successfully been accomplished to speeds of 20,000 rpm without any fluid loss because of the interface instability phenomena associated with the other foregoing seals. Investigation of this seal is continuing for the determina-

tion of the dimensional changes which may safely be made without affecting seal operation. It is intended that this investigation will be completed within the next reporting quarter.

11. Vacuum connection on the plain stationary wall

Vacuum connections were made on the plain stationary wall as shown in Configuration No. 6 on Figure 3. This allowed the observation of the seal surface while operating under a low pressure. The observation of the seal surface under a vacuum by the use of a strobe light revealed much outgassing from the water surface, which was determined to be boiling, because of the high vapor pressure of water. Therefore, no significant observations could be made and further work is required in this area. It is desirable when performing this additional work to use another working fluid such as a low vapor pressure oil.

12. Perpendicular outlets and plain stationary wall

Item No. 4 in Figure 3 shows a plain stationary wall with a perpendicular circular water outlet. This outlet and other similar outlets were installed in the wall to determine the effect of removing the water or working fluid at this particular point. Examination of the seal while in operation with a strobe light revealed that the outlet worked very well. There was no cavitation in the area of the outlet and pressure recovery was acceptable.

III. LIQUID METAL SEAL TEST RIG

Final quotations for the liquid metal seal test rig were received this reporting period. The low quotation was accepted after a visitation to the

vendor's facilities to insure that he was capable of maintaining the precision tolerances required. The order for manufacture was placed on June 12, 1963. Scheduled delivery was placed at 25 weeks.

The order for the test rig was placed without the finalized anti-sputtering configuration. This allowed the vendor to order all forgings and begin machining of the cold end of the spindle. This end requires the closest tolerance control, heat treatment and some welding and therefore, the longest time to manufacture. The seal configuration, or hot end of the test rig, will be finalized for manufacture by the end of October.

The test rig configuration is shown in Figure 4. The spindle configuration consists of three gas and one oil bearings supporting the shaft on which an airdriven power turbine is overhung from one end, and the seal test configuration is overhung from the other.

The gas bearings being utilized within the rig are, by their very nature, dependent on the maintenance of close radial clearance between the rotating shaft and stationary journal. Since the temperature of the hot end of the test rig will vary from room temperature to 1400°F during operation, the maintenance of close radial bearing clearance is dependent on the accurate prediction of the thermal expansion rates of the bearing shaft and journal. A successful design therefore, requires the use of materials with compatible thermal expansion rates and also an accurate knowledge of the internal temperature distribution within the shaft and housing.

A temperature distribution was calculated assuming a hot end temperature of 600 and 1400°F. These calculations were made utilizing a heat transfer program on the 7090 computer. The results of the calculations are shown in distribution plots on Figures 5 and 6. The bearing radial clearances were then calculated using temperature information and different materials. The calculations were made for 0.001, 0.0015 and 0.002-inch radial clearance in the cold condition. Considerations were also made for centrifugal growth of the shaft because of rotation. The data accumulated from these calculations was then used to make a final selection of test rig materials. The results of the clearance calculations on the selected Rex 49 shaft and the 316 SS housing are shown in Figures 7 through 12. The proposed gas bearings were designed utilizing this information.

1. Gas Bearing Design

The liquid metal seal test rig requirement for a reliable high speed low power consumption bearing could be met by the use of an externally pressurized hydrostatic pool bearing. Since the bearing was required to operate in close proximity with a vaporous alkali metal, it was necessary that the lubricating film be of an inert gas. Therefore, the bearing selected for use in the seal test rig will be used with argon. Argon will provide an inert covering for the liquid metal and also lubrication for the gas bearing. In addition to the foregoing problems, the temperature gradient found in the test rig was extreme. One end of the test rig was essentially at ambient temperature, whereas the other end was at 1400°F. Therefore, the differential expansion range of the shaft and bearing housing necessarily had to be properly accounted for if a successful design was to

be achieved. The gas bearing shaft was therefore broken up into three individual bearings, each of which had a length to diameter ratio of one.

Calculations on the gas bearing performance, as designed for the seal test rig, required establishment of criteria for their performance. Therefore, all calculations used to optimize the bearing were to meet the following criteria:

a. Maximize the gas bearing rigidity.

b. Maximize the bearing operating clearances between the rotating shaft and stationary journals.

c. Minimize the gas bearing argon flows since all flow used in the bearings would be discarded at the exit and not reclaimed for use.

With the foregoing criteria in mind it was necessary to perform careful analysis for the determination of the operating characteristics of the bearing system. The bearing system could be optimized by varying the following systems parameters. These parameters were:

a. The radial bearing clearance.

b. The axial bearing length and diameter.

c. The incoming supply pressure.

d. The outgoing discharge pressure.

e. The regulating supply orifice diameter in each bearing.

f. The bearing pool diameters and the bearing pool depth.

Before any actual design work could be accomplished it was necessary to select several parameters for the successful operation of the overall

test rig. Once these parameters were accepted the other parameters involved in the bearing design could be varied to form an optimum bearing system. Therefore, the shaft diameter and consequently, the bearing diameter were set at a value of three inches. This selection was not necessarily desirable from a bearing standpoint, however, it was necessary when considering the shaft critical speed and stiffness picture. A shaft of a larger or smaller size was not optimum from a vibration standpoint. This vibration analysis for the shaft was performed on an internal computer program and the first and second critical speeds were calculated and the shaft length and diameter, both external and internal, were optimized. With the bearing length to diameter ratio established as unity, the bearing length was then established at three inches.

These basic selections of the system allowed extensive calculations of the operating characteristics of the bearing system to be made. These calculations were very numerous and in all, several months work, utilizing an inplant computer program for the establishment of the bearing flows and bearing stiffnesses. A complete tabulation of the gas bearing data on the computer has been accumulated and is shown in Table I. The nomenclature used in the tabulation in Table I is listed within this report under the Symbols Section.

Referring to the tabulation of the bearing data it may be seen that the parameters which required specification were numerous and presented a difficult problem if an optimum solution was to be obtained. The gas bearing computer program calculated the bearing stiffness, bearing lubri-

cant flow and orifice diameter required when a specified pressure ratio of the internal pool pressure to supply pressure were maintained. This procedure was followed throughout the initial runs of the test program and the pressure ratio was maintained constant at 0.7. This allowed accumulation of data and subsequent evaluation to determine the approximate range of orifice diameters in the lubricate supply line.

Thereafter, the program was run utilizing the selected orifice diameters. The pressure ratio across the supply orifice was then calculated by the program along with the bearing stiffness and gas flows. From this information it was possible to plot various operating curves for an individual bearing.

Once the approximate orifice diameters and operating pressures were established, it was necessary to establish the optimum number of pools within the individual bearings. This optimization was done and established at three orifices. A comparison of the various orifice designs may be made by comparing an eight orifice bearing calculated in runs Number 22 through 25 and the three orifice bearing from all other runs accumulated in the tabulation.

The bearing pool diameters and pool depths required optimization before a bearing operating map could be made or before any attempt was made to optimize the overall bearing performance. The optimum pool dimensions were obtained by holding the other bearing parameters within the bearing program constant at their approximate values and calculating stiffness and

gas flow while varying pool dimensions. The results of these calculations are shown in Figures 13 and 14.

Figure 13 shows a plot of bearing stiffness and gas flow versus the bearing pool diameter. Analysis of the curves reveals that the bearing stiffness reaches a maximum in this particular design at a pool diameter of approximately 1-inch. The bearing flow may be seen to increase at a very steep rate under small pool diameters and approach a maximum and nearly constant value at a 1-inch pool diameter. This value of the pool diameter, although certainly not optimum from a flow standpoint, is optimum from a stiffness standpoint; therefore, the bearing pool diameters were established at 1-inch.

Figure 14 shows a plot of bearing stiffness and gas flow versus pool depth. Analysis of the curves reveals that the bearing stiffness approaches a maximum and remains constant thereafter for values of pool depth beyond 0.003 of an inch. The gas flow within the bearing is constantly increasing as the pool depth is varied; however, due to the inaccuracies in the program and the equations from which the program was derived, this flow curve should be partially disregarded. It may be seen from general gas laws that this increase in depth certainly does not increase the gas flow at such a rapid rate. The pool depth was established at 0.003 of an inch and this depth was maintained in all the individual pools and bearings.

By using the foregoing analysis of pool diameter and pool depth and the selected bearing diameter and bearing length, it was then possible to obtain plots and cross plots of bearing performance for various pressure ratios,

temperatures, inlet supply pressures and bearing clearances. The plots describing this analysis are included in Figures 13 through 28.

A typical plot of stiffness versus pressure ratio is shown in Figure 15. Analysis of this figure reveals that lines of constant bearing clearances and orifice diameters approach an optimum value at a pressure ratio of approximately 0.7. It may be seen that at lower pressure ratios the stiffness decreases but at a slower rate than the corresponding decrease at pressure ratios greater than 0.7.

From experience it is known that the operation of gas bearing at pressure ratios of 0.7 or less has been more successful than operation at pressure ratios greater than 0.7. This is caused by the potential energy within the pool being at a significantly higher value when the pressure ratio is greater than 0.7. For satisfactory bearing operation, the pressure ratio should always be maintained at a value lower than 0.7. A more significant plot has been prepared in Figures 16 through 19. These Figures show bearing stiffness plotted versus the gas temperature within the bearing. The effect of bearing supply pressure and radial clearance within the bearing is readily seen by evaluating these curves. It may be seen that increased supply pressures necessarily increase the stiffness of a given bearing whenever the pressure ratio is within a reasonable value of 0.5 to 0.8. Also, it may be seen that lower clearances within a given bearing of a particular design generally increase the bearing stiffnesses.

The above plots are especially important for use during operation of the test rig. When a particular gas temperature is measured within a

bearing and a particular flow pressure has been set, then by utilizing the bearing clearance as calculated from previous data, the approximate stiffness of the bearing system will be known. This is essential when operating the bearing since, should the bearing begin to run unstable, it may be immediately determined as to what the corrective action for stable operation should be. This correction may be made immediately and potentially damaging results may be avoided.

Figures 20 through 25 show plots of gas bearing flow versus pressure ratio within the bearing. These plots have been made for individual supply pressures and bearing temperatures. Analysis of these plots reveal increased flow requirements as supply orifice diameters increase, and when the internal bearing clearances are increased. It may be seen that this combination is in direct opposition to the desired operation from a stiffness standpoint; that is, maximum stiffnesses are generally obtainable from a gas bearing when gas lubricating flows are increased. However, it is necessary to optimize the overall system by compromising these parameters.

Figures 26 and 27 show plots of internal bearing clearances versus pool pressure ratios. These two figures have been plotted for constant orifice diameters on the inlet supply of 0.040 and 0.085 of an inch. The two plots show the possible operating range for the individual orifices with respect to supply pressure and bearing temperature. It may be seen that increased temperature causes the pressure ratio to change across a particular bearing as well as does the supply pressure. Therefore, throughout the operation of the test rig it will be necessary to monitor bearing temperature inasmuch as it will affect the running clearances or radial

clearances of the bearing and also the gas properties of the argon. The curves indicate the significant changes involved in an adjustment of the operating parameters.

Figure 28 shows a plot of bearing stiffness versus lubricant flow. This curve was made for a constant bearing radial clearance of 0.0015 of an inch and a constant pressure ratio of 0.7. Analysis of this plot reveals that bearing stiffness may be increased by simply increasing the bearing supply pressure provided the pressure ratio within the cavity is approximately 0.7. Also, an increase in gas temperature has the effect of decreasing the argon lubricant flow without affecting the bearing stiffnesses provided the bearing clearance remains constant. However, this picture is somewhat confused by the fact that the pressure ratio within the individual bearings changes significantly with changes in temperature and supply pressure. These changes are not reflected in their proper perspective by this particular plot since a constant orifice pressure ratio has been assumed.

When considering the operation of the gas bearing it must be remembered that the orifice selected to operate the bearing when it is initially started and obviously at lower temperatures must remain inside of the test rig throughout the particular test run even if the testing continues to extremely high temperatures. There is no convenient method available to change the operating orifices while the test rig is running. Therefore, the pressure ratio effect must be accounted for before initiation of a long time test by selecting the proper supply orifice that will provide acceptable running throughout the operating spectrum.

A complete summary of the clearance data, orifice sizing, gas bearing stiffness and orifice pressure ratio is shown in Table II. In this table, the clearance data has been established from the thermal expansion data previously discussed and the bearing operation has been predicted for various operating temperatures which are expected within the test rig. Based on these predictions, the appropriate orifice for test rig operation has been selected, accounting for optimum stiffness and orifice pressure ratios. The flow within the gas bearing has been maintained at an acceptable limit as dictated by the supply facility established in Building 314. These calculations have been made for all three of the individual gas bearings. It may be seen from this tabulation that the requirements of the individual bearings along the test rig vary considerably in their requirements for orifice sizes and the resultant stiffnesses and pressure ratios.

2. MATERIALS SUPPORT

Investigation of the materials being used in the test rig was made to determine their effect on the operation of the close tolerance gas bearing. It was necessary that the materials demonstrate high strength at elevated temperatures and good dimensional stability. Various anti-seize coatings were also evaluated to insure ease of disassembly after operation at high temperatures required by the proposed testing.

Rex 49 Alloy Tensile and Creep Strength

Tensile tests to 1400°F in flowing argon have been completed on Rex 49. The test bars were hardened and drawn to Rc 56 before finish grinding to 0.160" gauge diameter. The results of the testing are shown below.

Tensile Properties of Rex 49

Average of Two Specimens .005 in/in/min Strain Rate

Test Temperature	ULT (Ksi)	.2% YS (Ksi)	% El	% R.A.
RT	277.5	240.5	0.0	0.0
600°F	271.7	238.7	1.4	2.0
800°F	253.5	216.0	1.7	2.9
1000°F	205.0	177.0	1.9	2.5
1200°F	148.7	114.3	1.5	1.0
1400°F	46.7	31.8	25.2	63.9

The room temperature test specimens failed in the threads. The threaded sections were cut off and the bars pulled using the button-head specimen adapters.

The 1000 hour creep tests are being conducted at the General Electric Company's Advanced Technology Laboratory. Tests to be performed will be conducted as follows:

Test Temperature	Stress Level
800°F	140 Ksi
1200°F	15 Ksi
1400°F	2.4 Ksi

These test conditions are based on the Larson-Miller plot of preliminary creep data. Preliminary testing recorded rupture times of 8.51 hours at 15 Ksi stress and 1200°F. The average creep rate over 400 hours was 6×10^{-5} in/in-hr at 100 Ksi and 800°F. This specimen was step loaded to 140 Ksi for an additional 100 hours without failing.

Dimensional Stability of Type 316 Stainless Steel

The dimensional stability of 1/2 inch mill annealed rod was measured after exposure to 600, 800 and 1000°F temperatures for 100 and 1000 hours in vacuum. The results of the testing are summarized below. Two specimens were treated simultaneously.

Heat Treatment	Shrinkage Rate Microinch/inch/hr.	
600°F - 100 hrs.	1.27	1.31
600°F - 1000 hrs.	0.188	0.194
800°F - 100 hrs.	2.33	2.25
800°F - 1000 hrs.	0.040	0.236
1000°F - 100 hrs.	1.67	1.60
1000°F - 1000 hrs.	0.150	0.113

These data indicate that shrinkage occurred primarily during the first 100 hours of testing. Therefore, for gas bearing applications, it is necessary to perform a 100 hour heat treatment at 800 to 1000°F prior to final machining.

Dimensional Stability of Rex 49

The dimensional stability of Rex 49 was obtained after exposure to 600, 800 and 1000°F temperatures for 250, 500 and 1000 hours. The results of two samples are summarized below.

Heat Treatment	Shrinkage Rate Microinch/inch/hr
600°F - 500 hrs.	0.010
600°F - 1000 hrs.	0.006
800°F - 500 hrs.	0.016
800°F - 1000 hrs.	0.005
1000°F - 250 hrs.	- 0.168 (growth)
1000°F - 500 hrs.	- 0.064 (growth)

These data indicate that growth occurs at elevated temperatures, but the material is still acceptable for gas bearing applications.

Anti-Seize Coatings for Type 316 Stainless Steel

The anti-galling and anti-seizing properties of various electroplates and of lubricants as applied either singly or in combination to 316 Stainless Steel bolts have been evaluated after exposure to 1200°F for 100 hours. The results of the testing are summarized below.

	Original Torque	Breakaway Torque
Silver Plate	100	160
0.00075 inch thick	100	160
Copper Plate	100	240
0.001 inch thick	100	200
Silver Plate Plus	100	160
MgO in. Xylene	100	120
Copper Plate Plus	100	140
MgO in. Xylene	100	120
Mgo in Xylene	100	140
	100	130
"Led" Plate Compound	100	220
	100	190
Nickel Powder	100	120
	100	90

No galling or seizing was observed using any of these coatings. The magnesium oxide slurry appears to be the most acceptable coating because of the low breakaway torque observed and because of the ease of reapplying.

Electron Beam Welding of Rex 49

Initial welding of annealed Rex 49 specimens indicated a crack sensitivity of incomplete weld penetration occurred. However, it was demonstrated that

the cracked welds could be "repair welded" successfully following a first temper of the initial weld.

Additional welding information is being obtained to determine Rex 49 weldability in a hardened condition.

III. LIQUID METAL SEAL TEST FACILITY

Design work on the liquid metal seal test facility has been completed and all materials and purchased items have been received. Requests for quotation on assembly of the facility as a self-contained package were sent to a number of qualified vendors this month. These quotations have been received and selection of the low bidder has been completed. The assembly order for the seal test facility package has been placed. Delivery of the facility is scheduled for October 23, 1963.

Bids for installation of the facility in Building 314 at Evendale are now being accepted. It is intended that the installation of the facility will take four weeks. This schedule allows check-out of the loop and test rig to start by the middle of November. This facility will be capable of providing the follcwing services.

1. Liquid potassium at melting point to 1400 F^{o} temperature.
2. Argon flow for gas bearing lubrication at a rate up to 200 lb/hr and 200 psi pressure.
3. Vacuum on the low pressure side of the dynamic seal down to 10^{-6} mm of mercury absolute.
4. Air at a rate of 2 lb/sec to power the air turbine drive.

Instrumentation for monitoring the operation of the test rig performance has been detailed, the instruments ordered and presently on hand. These instruments are separate from those monitoring the liquid metal facility and shown on the schematic in the third quarterly report. The following is a list of the procured instrumentation available for data acquisitions

Quantity	
1	8-Channel Sanborn Recorder
1	Frequency Meter Preamplifier
4	Carrier Preamplifier
3	Low Level Preamplifier
2	Pressure Scanners
2	Pressure Scanner Control Units
12	160 psi Test Gauge
2	100 psi Test Gauge
1	Distance Detector Energizer
2	Distance Detectors
1	Calibrated Furnace
1	10 lb Load Cell
1	Sixty Point Recorder
1	Overspeed Trip

SYMBOLS

N	=	number of orifices
G	=	gravitational constant, in/sec^2
D	=	bearing diameter, in.
BL	=	bearing length, in.
SH	=	radial clearance, in.
DP	=	pool diameter, in.
HP	=	pool depth, in.
CD	=	discharge coefficient
T	=	temperature, ^oR
U	=	viscosity, $(lb/sec)/in.^2$
AK	=	ratio of specific heats C_p/C_v
R	=	gas constant, $in.^2/(sec^2\ ^oR)$
PE	=	ambient pressure, psia
P1	=	supply pressure, psia
PR	=	optimum ratio of pool pressure to supply pressure (eccentricity ratio = 0)
TOL	=	pool pressure tolerance, psi
EPI	=	initial eccentricity ratio
EP2	=	final eccentricity ratio
DEP	=	delta (increment) eccentricity ratio
AA	=	orifice diameter, in.
K	=	stiffness, lb/in.
P_r	=	pool pressure, $lb/in.^2$
W	=	flow per orifice, lb/sec.
W_1	=	flow per bearing, lb/sec.
W_2	=	flow per two bearings, lb/sec.
$W_2{}_1$	=	flow per two bearings, lb/hr.

TABLE I

RUN NO.	N	G	DP	$Ux10^{-9}$	P1	EP2	D	HP	AK	PR	DEP	BL	CD	$Rx10^{5}$	TOL	AA	SH	T	t	PE	EPI	K	P_r	W	W_1	W_2	W_2^1
8	3	386	1.00	3.59	115	1.00	3.00	.003	1.67	0.70	0.2	3.00	0.80	1.792	0.10	0.129	.0015	600	140	20	-1.00	293,000	80.4	.00412	.01236	.02472	89.0
9	3	386	1.00	6.58	115	1.00	3.00	.003	1.67	0.70	0.2	3.00	0.80	1.792	0.10	0.046	.0015	1400	940	20	-1.00	294,000	80.5	.000964	.00289	.00578	20.8
10	3	386	1.00	3.59	165	1.00	3.00	.003	1.67	0.70	0.2	3.00	0.80	1.792	0.10	0.065	.001	600	140	20	-1.00	672,000	115.5	.00262	.00786	.01572	56.6
11	3	386	1.00	3.59	115	1.00	3.00	.003	1.67	0.70	0.2	3.00	0.80	1.792	0.10	0.276	.002	600	140	20	-1.00	212,000	80.5	.00977	.02931	.05862	211.0
12	3	386	1.00	3.59	165	1.00	3.00	.003	1.67	0.70	0.2	3.00	0.80	1.792	0.10	0.413	.002	600	140	20	-1.00	315,000	115.5	.021	.063	.126	453.0
13	3	386	1.00	6.58	115	1.00	3.00	.003	1.67	0.70	0.2	3.00	0.80	1.792	0.10	0.015	.001	1400	940	20	-1.00	455,000	80.5	.000285	.000855	.001710	6.2
14	3	386	1.00	3.59	115	1.00	3.00	.003	1.67	0.70	0.2	3.00	0.80	1.792	0.10	0.043	.001	600	140	20	-1.00	455,000	80.5	.00122	.00366	.00732	26.3
15	3	386	1.00	6.58	165	1.00	3.00	.003	1.67	0.70	0.2	3.00	0.80	1.792	0.10	0.023	.001	1400	940	20	-1.00	675,000	115.5	.000613	.001839	.00368	13.3
17	3	386	1.00	3.59	90	1.00	3.00	.003	1.67	0.70	0.2	3.00	0.80	1.792	0.10	0.096	.0015	600	140	20	-1.00	220,000	62.9	.00239	.00717	.01434	39.9
18	3	386	1.00	3.59	90	1.00	3.00	.003	1.67	0.70	0.2	3.00	0.80	1.792	0.10	0.204	.002	600	140	20	-1.00	162,000	62.9	.00566	.01700	.0340	94.5
19	3	386	1.00	3.59	65	1.00	3.00	.003	1.67	0.70	0.2	3.00	0.80	1.792	0.10	0.020	.001	600	140	20	-1.00	230,000	45.5	.000319	.000956	.00191	5.3
20	3	386	1.00	3.59	65	1.00	3.00	.003	1.67	0.70	0.2	3.00	0.80	1.792	0.10	0.060	.0015	600	140	20	-1.00	147,000	45.5	.00108	.00324	.00648	18.0
21	3	386	1.00	3.59	65	1.00	3.00	.003	1.67	0.70	0.2	3.00	0.80	1.792	0.10	0.127	.002	600	140	20	-1.00	105,000	45.5	.00255	.00765	.0153	42.5
22	8	386	0.100	3.59	165	1.00	3.00	.0001	1.67	0.70	0.2	3.00	0.80	1.792	0.10	0.072	.001	600	140	20	-1.00	550,000	115.5	.000807	.00646	.01292	35.9
23	8	386	0.100	3.59	165	1.00	3.00	.0001	1.67	0.70	0.2	3.00	0.80	1.792	0.10	0.167	.0015	600	140	20	-1.00	370,000	115.5	.00272	.0218	.0436	121.0
24	8	386	0.100	3.59	165	.00	3.00	.0001	1.67	0.70	0.2	3.00	0.80	1.792	0.10	0.302	.002	600	140	20	-1.00		115.5	.00645	.0516	.1032	287.0
25	8	386	0.100	3.59	90	1.00	3.00	.0001	1.67	0.70	0.2	3.00	0.80	1.792	0.10		.0015	600	140	20	-1.00						
27	3	386	1.00	5.27	165	1.00	3.00	.003	1.67	.655	0.2	3.00	0.80	1.792	0.10	.085	0.0015	1000	540	20	-1.00	436,000	108	.00314			
28	3	386	1.00	3.59	165	1.00	3.00	.003	1.67	.497	0.2	3.00	0.80	1.792	0.10	.085	0.0015	600	140	20	-1.00	388,000	82	.00429			
29	3	386	1.00	7.26	115	1.00	3.00	.003	1.67	.870	0.2	3.00	0.80	1.792	0.10	.085	0.0015	1600	1140	20	-1.00	212,000	100	.00121			
30	3	386	1.00	3.59	115	1.00	3.00	.003	1.67	.600	0.2	3.00	0.80	1.792	0.10	.085	0.0015	600	140	20	-1.00	291,000	69	.00292			
31	3	386	1.00	7.26	65	1.00	3.00	.003	1.67	.952	0.2	3.00	0.80	1.792	0.10	.085	0.0015	1600	1140	20	-1.00	53,700	62	.00043			
32	3	386	1.00	3.59	65	1.00	3.00	.003	1.67	.768	0.2	3.00	0.80	1.792	0.10	.085	0.0015	600	140	20	-1.00	142,000	50	.00139			
33	3	386	1.00	7.26	165	1.00	3.00	.003	1.67	.673	0.2	3.00	0.80	1.792	0.10	.085	0.0018	1600	1140	20	-1.00	355,000	111	.00261			
34	3	386	1.00	5.27	165	1.00	3.00	.003	1.67	.533	0.2	3.00	0.80	1.792	0.10	.085	0.0018	1000	540	20	-1.00	336,000	88	.0053			
35	3	386	1.00	3.59	165	1.00	3.00	.003	1.67	.401	0.2	3.00	0.80	1.792	0.10	.085	0.0018	600	140	20	-1.00	255,000	66	.00458			
36	3	386	1.00	7.26	115	1.00	3.00	.003	1.67	.774	0.2	3.00	0.80	1.792	0.10	.085	0.0018	1600	1140	20	-1.00	224,000	89	.00162			

TABLE I (Continued)

RUN NO.	N	G	DP	Ux10^{-9}	P1	EP2	D	HP	AK	PR	DEP	BL	CD	Rx10^{5}	TOL	AA	SH	T	E	PE	EP1	K	P	M
37	3	386	1.00	3.59	115	1.00	3.00	.003	1.67	.487	0.2	3.00	0.80	1.792	0.10	.085	0.008	600	140	20	-1.00	206,000	56	.00319
38	3	386	1.00	7.26	65	1.00	3.00	.003	1.67	.908	0.2	3.00	0.80	1.792	0.10	.085	0.0018	1600	1140	20	-1.00	77,400	59	.00065
39	3	386	1.00	3.59	65	1.00	3.00	.003	1.67	.678	0.2	3.00	0.80	1.792	0.10	.085	0.0018	600	140	20	-1.00	117,000	44	.00167
40	3	386	1.00	7.26	165	1.00	3.00	.003	1.67	.951	0.2	3.00	0.80	1.792	0.10	.085	0.0010	1600	1140	20	-1.00	212,000	158	.000926
41	3	386	1.00	5.27	165	1.00	3.00	.003	1.67	.897	0.2	3.00	0.80	1.792	0.10	.085	0.0010	1000	540	20	-1.00	423,000	148	.00178
42	3	386	1.00	3.59	165	1.00	3.00	.003	1.67	.770	0.2	3.00	0.80	1.792	0.10	.085	0.0010	600	140	20	-1.00	634,000	127	.00318
43	3	386	1.00	7.26	115	1.00	3.00	.003	1.67	.983	0.2	3.00	0.80	1.792	0.10	.085	0.0010	1600	1140	20	-1.00	82,000	113	.000465
44	3	386	1.00	3.59	115	1.00	3.00	.003	1.67	.853	0.2	3.00	0.80	1.792	0.10	.085	0.0010	600	140	20	-1.00	350,000	98	.00186
45	3	386	1.00	7.26	65	1.00	3.00	.003	1.67	1.000	0.2	3.00	0.80	1.792	0.10	.085	0.0010	1600	1140	20	-1.00	13,000	65	.000143
46	3	386	1.00	3.59	65	1.00	3.00	.003	1.67	.938	0.2	3.00	0.80	1.792	0.10	.085	0.0010	600	140	20	-1.00	97,000	61	.000669
47	3	386	1.00	7.26	115	1.00	3.00	.003	1.67	.913	0.2	3.00	0.80	1.792	0.10	.110	0.0015	1600	1140	20	-1.00	168,000	105	.00134
48	3	386	1.00	3.59	115	1.00	3.00	.003	1.67	.661	0.2	3.00	0.80	1.792	0.10	.110	0.0015	600	140	20	-1.00	293,000	76	.00363
49	3	386	1.00	7.26	65	1.00	3.00	.003	1.67	.970	0.2	3.00	0.80	1.792	0.10	.110	0.0015	1600	1140	20	-1.00	37,000	61	.0045
50	3	386	1.00	3.59	65	1.00	3.00	.003	1.67	.831	0.2	3.00	0.80	1.792	0.10	.110	0.0015	600	140	20	-1.00	129,000	54	.00163
51	3	386	1.00	7.26	165	1.00	3.00	.003	1.67	.709	0.2	3.00	0.80	1.792	0.10	.060	0.0015	1600	1140	20	-1.00	430,000	117	.00167
52	3	386	1.00	3.59	165	1.00	3.00	.003	1.67	.422	0.2	3.00	0.80	1.792	0.10	.060	0.0015	600	140	20	-1.00	345,000	70	.00303
53	3	386	1.00	3.59	115	1.00	3.00	.003	1.67	.522	0.2	3.00	0.80	1.792	0.10	.060	0.0015	600	140	20	-1.00	262,000	60	.00211
54	3	386	1.00	7.26	65	1.00	3.00	.003	1.67	.923	0.2	3.00	0.80	1.792	0.10	.060	0.0015	1600	1140	20	-1.00	82,000	60	.00039
55	3	386	1.00	3.59	65	1.00	3.00	.003	1.67	.707	0.2	3.00	0.80	1.792	0.10	.060	0.0015	600	140	20	-1.00	144,000	46	.00108
56	3	386	0.5	3.59	115	1.00	3.00	.003	1.67	.712	0.2	3.00	0.80	1.792	0.10	.085	0.0015	600	140	20	-1.00	250,000	82	.00268
57	3	386	1.5	3.59	115	1.00	3.00	.003	1.67	.504	0.2	3.00	0.80	1.792	0.10	.085	0.0015	600	140	20	-1.00	260,000	58	.00299
58	3	386	1.0	3.59	115	1.00	3.00	.001	1.67	.469	0.2	3.00	0.80	1.792	0.10	.085	0.0015	600	140	20	-1.00	215,000	54	.00166
59	3	386	1.0	3.59	115	1.00	3.00	.006	1.67	.722	0.2	3.00	0.80	1.792	0.10	.085	0.0015	600	140	20	-1.00	310,000	83	.00441
60	3	386	1.00	7.26	165	1.00	3.00	.003	1.67	0.79	0.2	3.00	0.80	1.792	0.10	.085	.0015	1600	1140	20	-1.00	400,000	130.2	.0021
61	3	386	1.00	5.27	115	1.00	3.00	.003	1.67	0.75	0.2	3.00	0.80	1.792	0.10	.085	.0015	1000	540	20	-1.00	282,000	86.6	.0020
62	3	386	1.00	5.27	115	1.00	3.00	.003	1.67	0.64	0.2	3.00	0.80	1.792	0.10	.085	.0018	1000	540	20	-1.00	243,000	73.1	.0024
63	3	386	1.00	5.27	115	1.00	3.00	.003	1.67	0.94	0.2	3.00	0.80	1.792	0.10	.085	.0010	1000	540	20	-1.00	188,000	108.3	.0010

TABLE I (Continued)

RUN NO.	N	G	DP	$Ux10^{-9}$	P1	EP2	D	HP	AK	PR	DEP	BL	CD	$Rx10^{5}$	TOL	AA	SH	T	t	PE	EP1	K	P	W
64	3	386	1.00	3.59	65	1.00	3.00	.003	1.67	0.84	0.2	3.00	0.80	1.792	0.10	.040	.0010	600	140	20	-1.00	191,000	54.7	.00051
65	3	386	1.00	7.26	65	1.00	3.00	.003	1.67	0.97	0.2	3.00	0.80	1.792	0.10	.040	.0010	1600	1140	20	-1.00	52,000	63.3	.00013
66	3	386	1.00	3.59	115	1.00	3.00	.003	1.67	0.68	0.2	3.00	0.80	1.792	0.10	.040	.0010	600	140	20	-1.00	455,000	78.4	.00115
67	3	386	1.00	5.27	115	1.00	3.00	.003	1.67	0.83	0.2	3.00	0.80	1.792	0.10	.040	.0010	1000	540	20	-1.00	378,000	95.3	.00072
68	3	386	1.00	7.26	115	1.00	3.00	.003	1.67	0.92	0.2	3.00	0.80	1.792	0.10	.040	.0010	1600	1140	20	-1.00	234,000	105.8	.00041
69	3	386	1.00	3.59	165	1.00	3.00	.003	1.67	0.58	0.2	3.00	0.80	1.792	0.10	.040	.0010	600	140	20	-1.00	682,000	95.6	.00176
70	3	386	1.00	5.27	165	1.00	3.00	.003	1.67	0.74	0.2	3.00	0.80	1.792	0.10	.040	.0010	1000	540	20	-1.00	650,000	122.1	.00120
71	3	386	1.00	7.26	165	1.00	3.00	.003	1.67	0.86	0.2	3.00	0.80	1.792	0.10	.040	.0010	1600	1140	20	-1.00	490,000	142.0	.00075
72	3	386	1.00	3.59	65	1.00	3.00	.003	1.67	0.62	0.2	3.00	0.80	1.792	0.10	.040	.0015	600	140	20	-1.00	137,000	40.3	.00077
73	3	386	1.00	7.26	65	1.00	3.00	.003	1.67	0.86	0.2	3.00	0.80	1.792	0.10	.040	.0015	1600	1140	20	-1.00	116,000	55.8	.00033
74	3	386	1.00	3.59	115	1.00	3.00	.003	1.67	0.44	0.2	3.00	0.80	1.792	0.10	.040	.0015	600	140	20	-1.00	227,000	50.5	.00141
75	3	386	1.00	5.27	115	1.00	3.00	.003	1.67	0.57	0.2	3.00	0.80	1.792	0.10	.040	.0015	1000	540	20	-1.00	287,000	65.7	.00107
76	3	386	1.00	7.26	115	1.00	3.00	.003	1.67	0.71	0.2	3.00	0.80	1.792	0.10	.040	.0015	1600	1140	20	-1.00	295,000	81.1	.00078
77	3	386	1.00	3.59	165	1.00	3.00	.003	1.67	0.36	0.2	3.00	0.80	1.792	0.10	.040	.0015	600	140	20	-1.00	274,000	58.6	.00202
78	3	386	1.00	5.27	165	1.00	3.00	.003	1.67	0.47	0.2	3.00	0.80	1.792	0.10	.040	.0015	1000	540	20	-1.00	380,000	77.8	.00156
79	3	386	1.00	7.26	165	1.00	3.00	.003	1.67	0.60	0.2	3.00	0.80	1.792	0.10	.040	.0015	1600	1140	20	-1.00	442,000	99.5	.00120
80	3	386	1.00	3.59	165	1.00	3.00	.003	1.67	0.68	0.2	3.00	0.80	1.792	0.10	.060	.0010	600	140	20	-1.00	683,000	112.5	.00248
81	3	386	1.00	3.59	165	1.00	3.00	.003	1.67	0.34	0.2	3.00	0.80	1.792	0.10	.060	.0018	600	140	20	-1.00	224,000	56.7	.00323
82	3	386	1.00	3.59	115	1.00	3.00	.003	1.67	0.78	0.2	3.00	0.80	1.792	0.10	.060	.0010	600	140	20	-1.00	418,000	89.5	.00153
83	3	386	1.00	3.59	115	1.00	3.00	.003	1.67	0.43	0.2	3.00	0.80	1.792	0.10	.060	.0018	600	140	20	-1.00	177,000	49.0	.00225

TABLE II

BEARING NUMBER	HOT END TEMP °F	BEARING TEMP °R	BEARING CLEARANCE (inch	ORIFICE DIAMETER, inch at SUPPLY PRESSURE - psia 165	115	65	STIFFNESS, lb/inch at SUPPLY PRESSURE - psia 165	115	65	ORIFICE PRESSURE RATIO at SUPPLY PRESSURE - psia 165	115	65
I	140°	600°	0.0017	>0.085	>0.085	0.085	290,000	230,000	122,000	0.43	0.52	0.7
	600°	700°	0.0018	>0.085	>0.085	0.085	274,000	210,000		0.43	0.52	0.7
	1400°	920°	0.00129	0.060	0.060	<.040	430,000	350,000		0.7	0.68	>.75
II	140°	600°	0.0015	>0.085	>0.085	0.06	389,000	293,000	142,000	0.49	0.6	0.71
	600°	740°	0.00152	>0.085	>0.085	(.085≯0.040)	330,000	250,000	125,000	0.45	0.55	0.72
	1400°	1060°	0.00147	0.085	0.060	0.04	440,000	350,000	130,000	0.67	0.63	0.75
III	140°	600°	0.0015	>0.085	>0.085	0.06	389,000	293,000	142,000	0.49	0.6	0.71
	600°	820°	0.00162	>0.085	0.085	0.04	390,000	280,000	160,000	0.57	0.68	0.66
	1400°	1260°	0.0015	0.085	0.060	<0.04	443,000	370,000	130,000	0.71	0.6	0.74

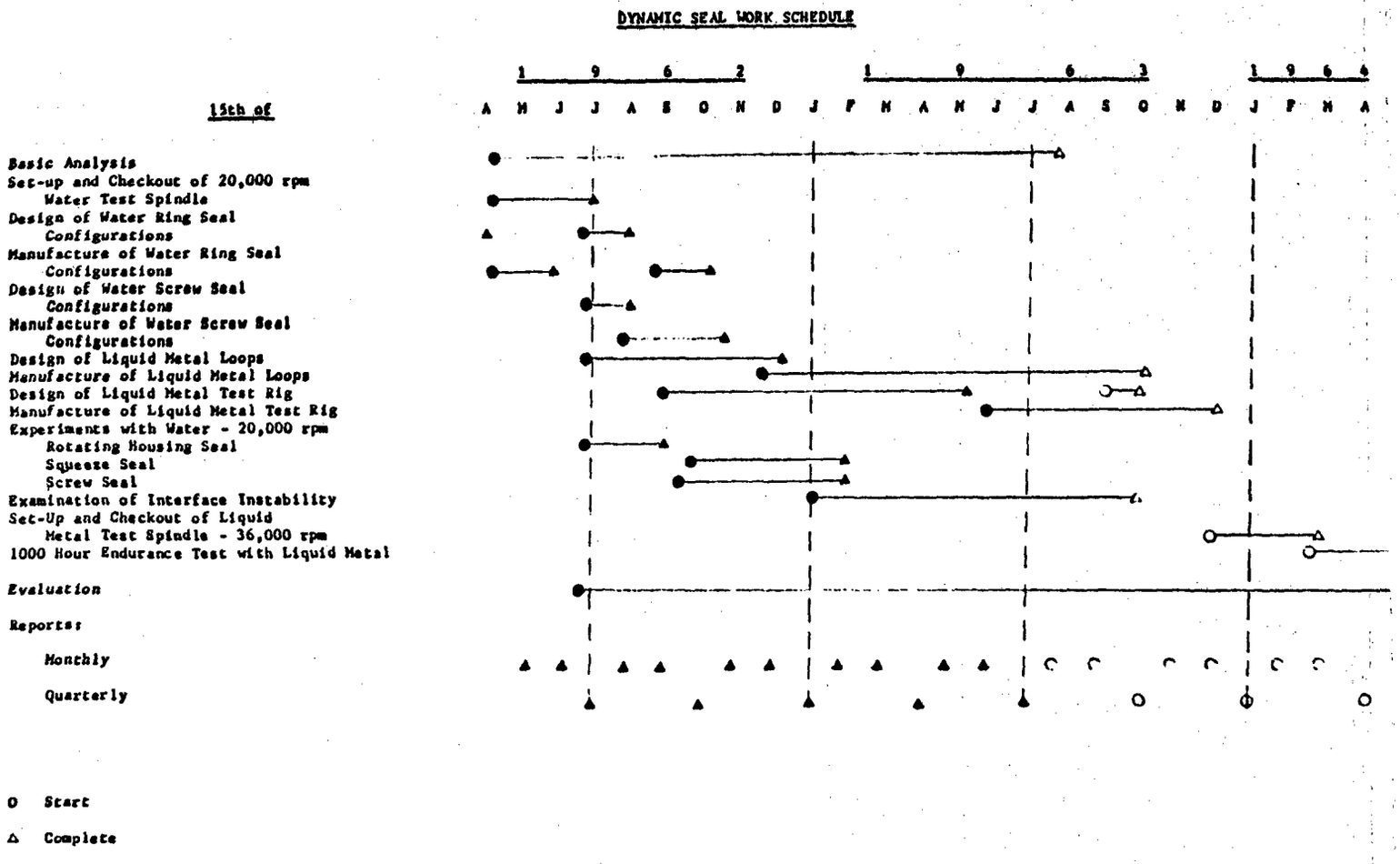

Figure 1. Dynamic Seal Work Schedule

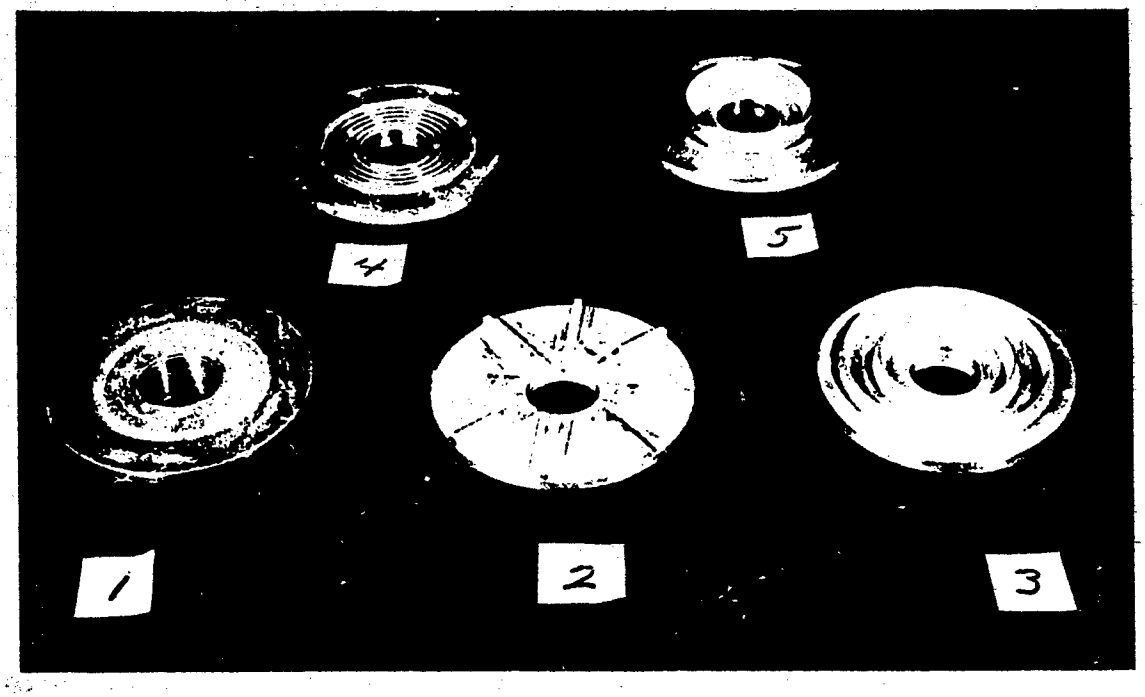

Figure 2. Rotating Disk Configurations

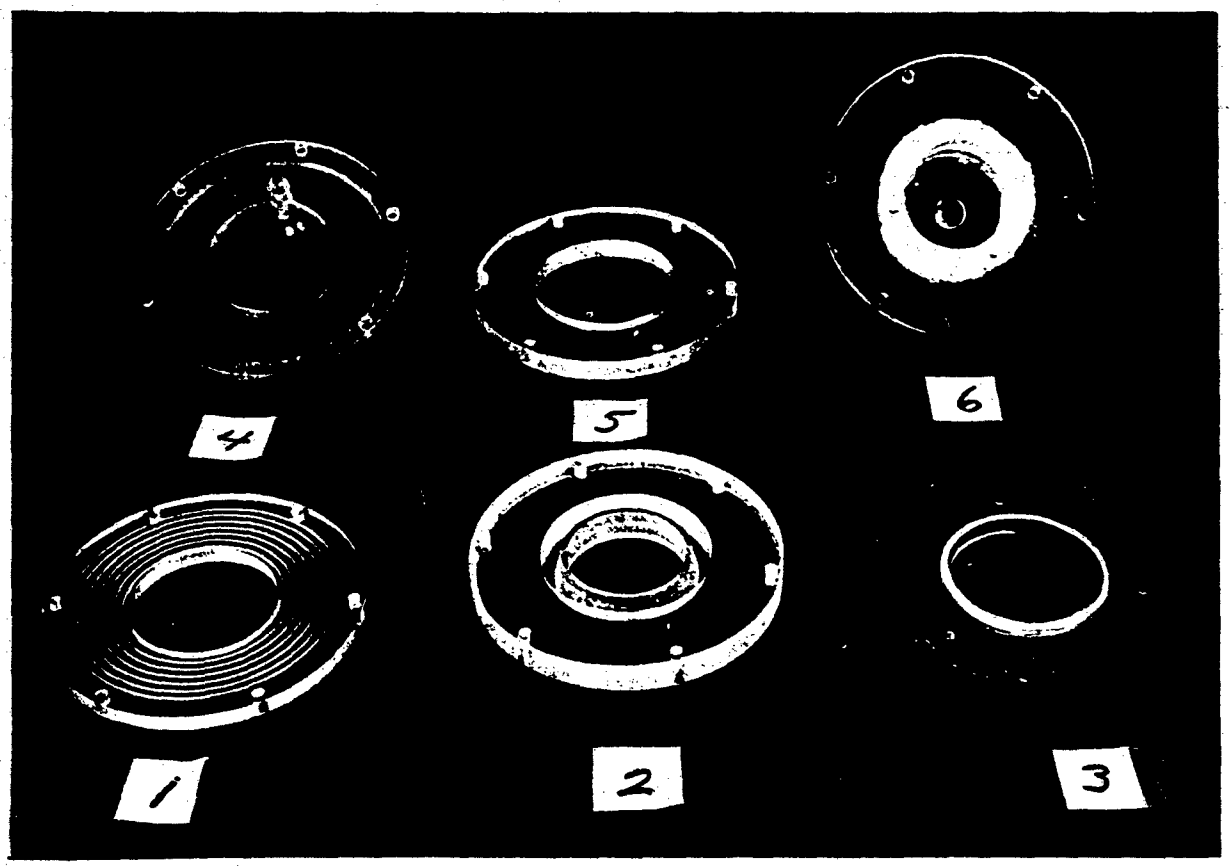

Figure 3. Rotating Disk Configurations

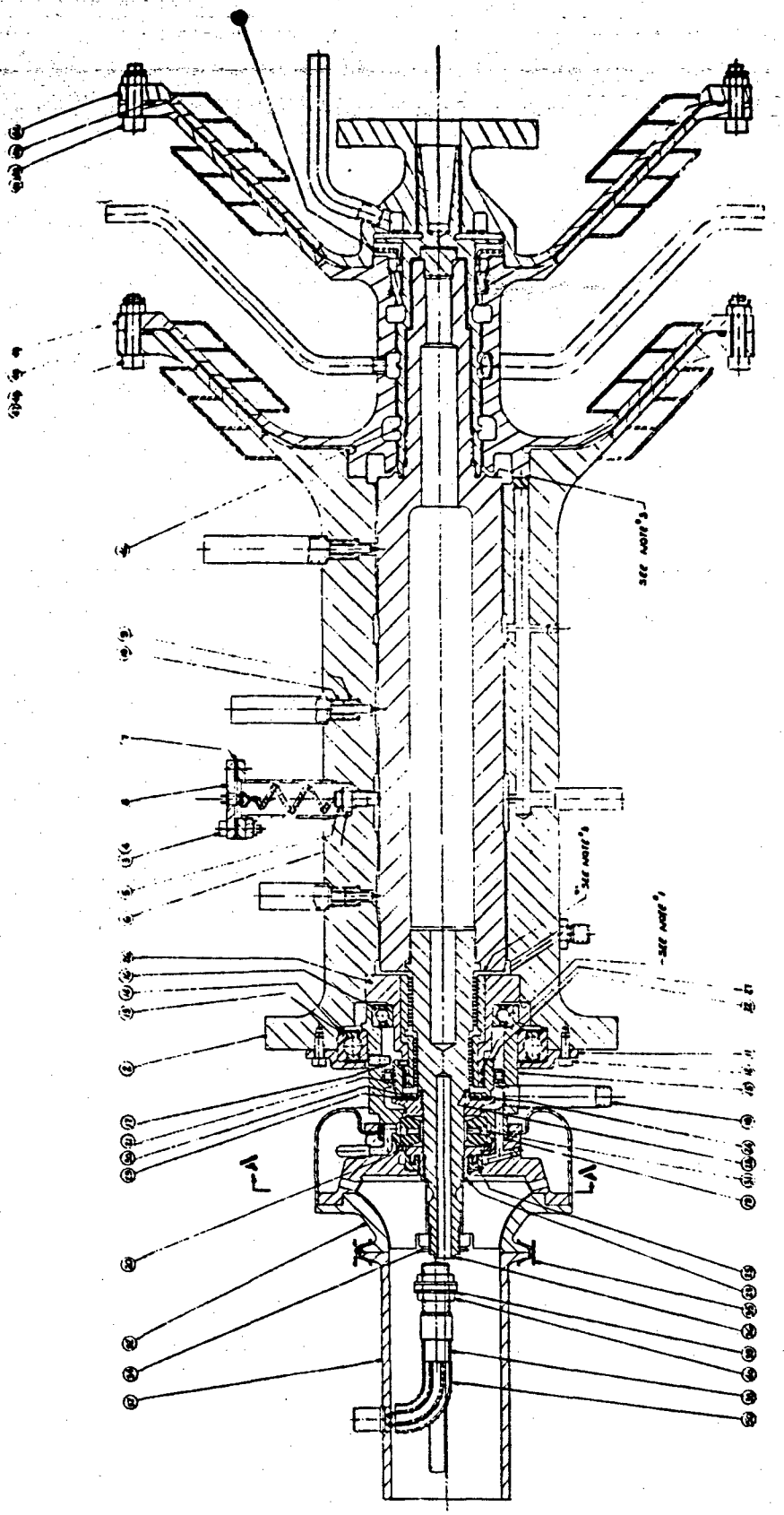

Figure 4. Liquid Metal Test Rig

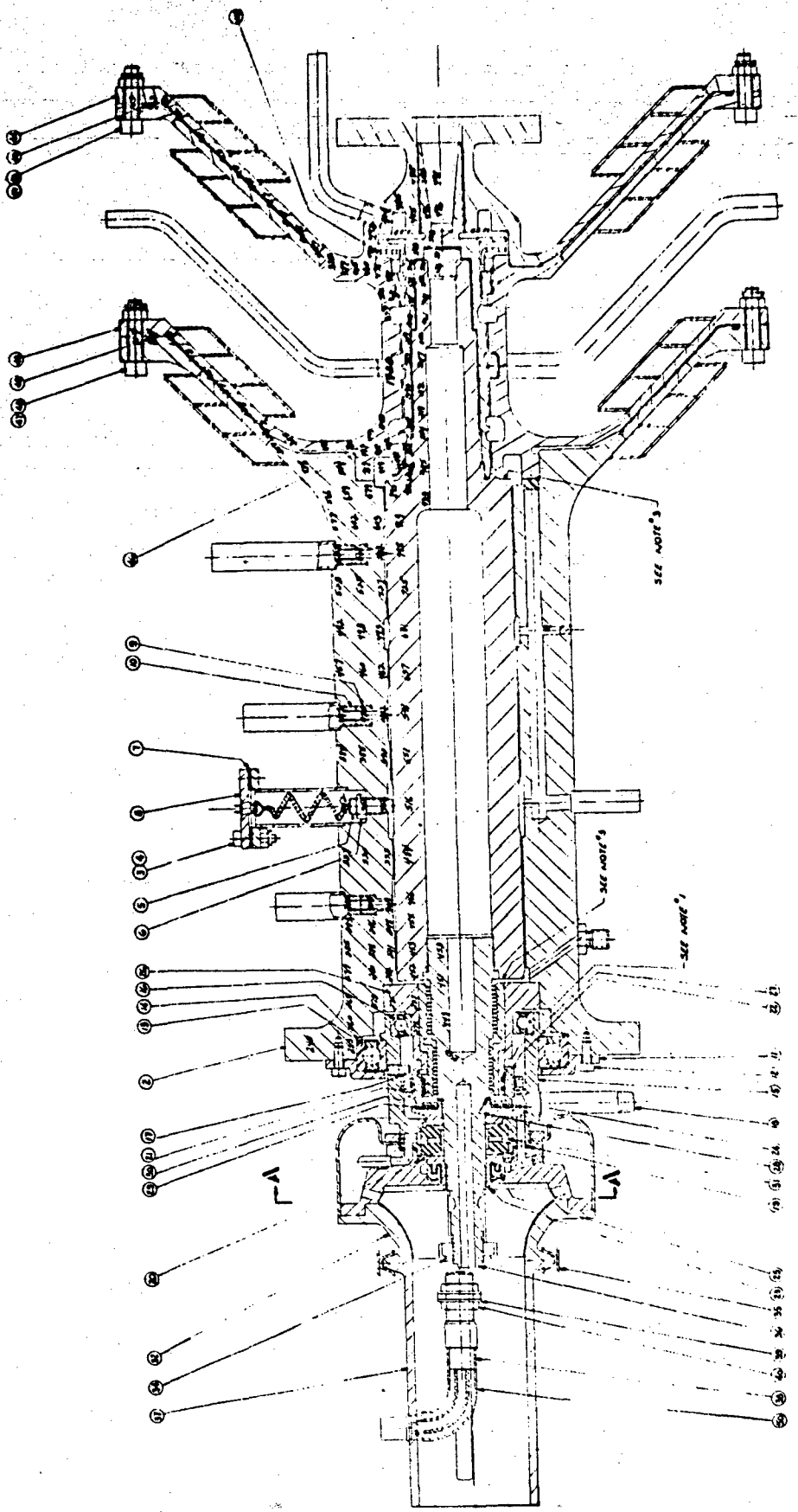

Figure 5. 1400°F Temperature Distribution

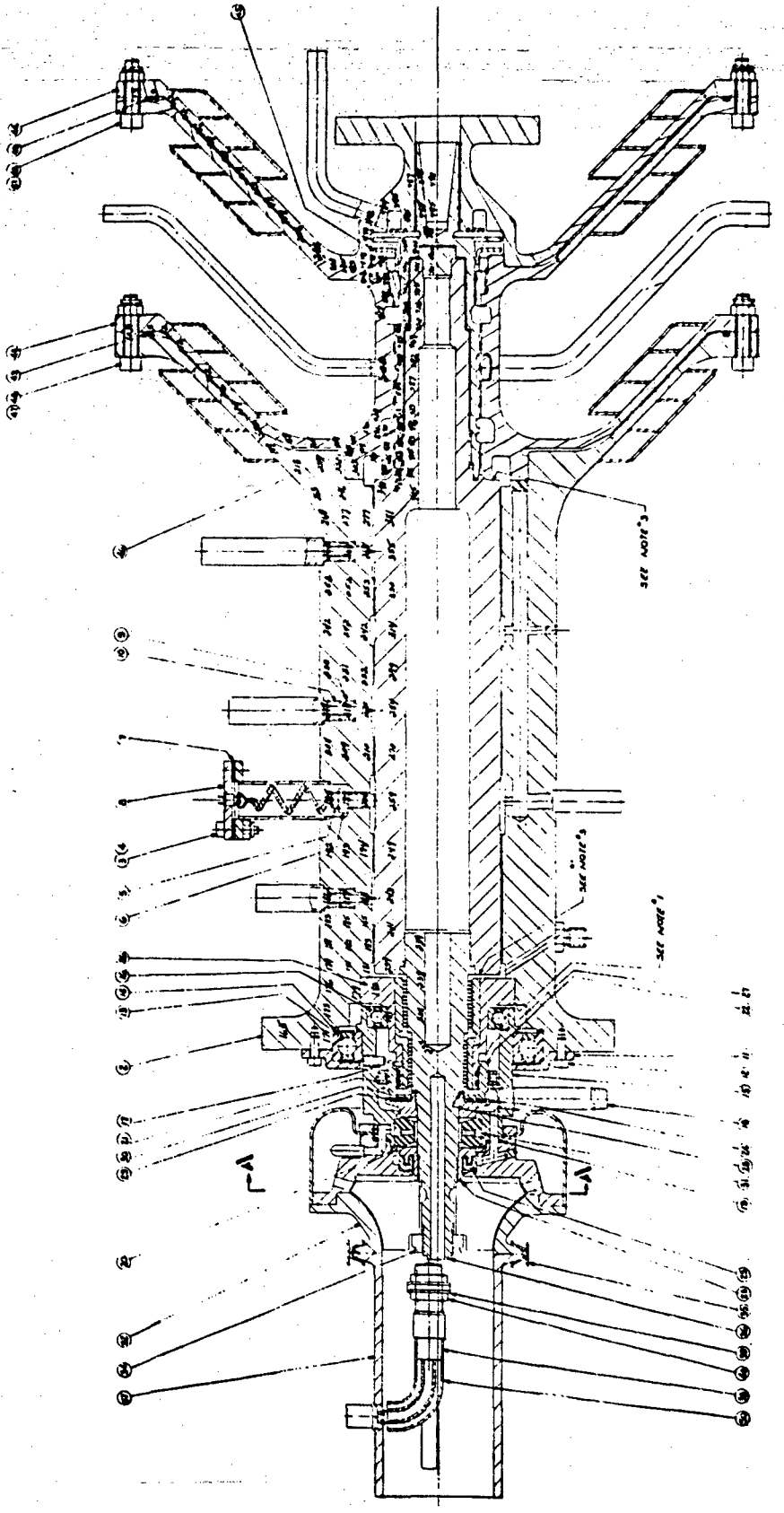

Figure 6. 600°F Temperature Distribution

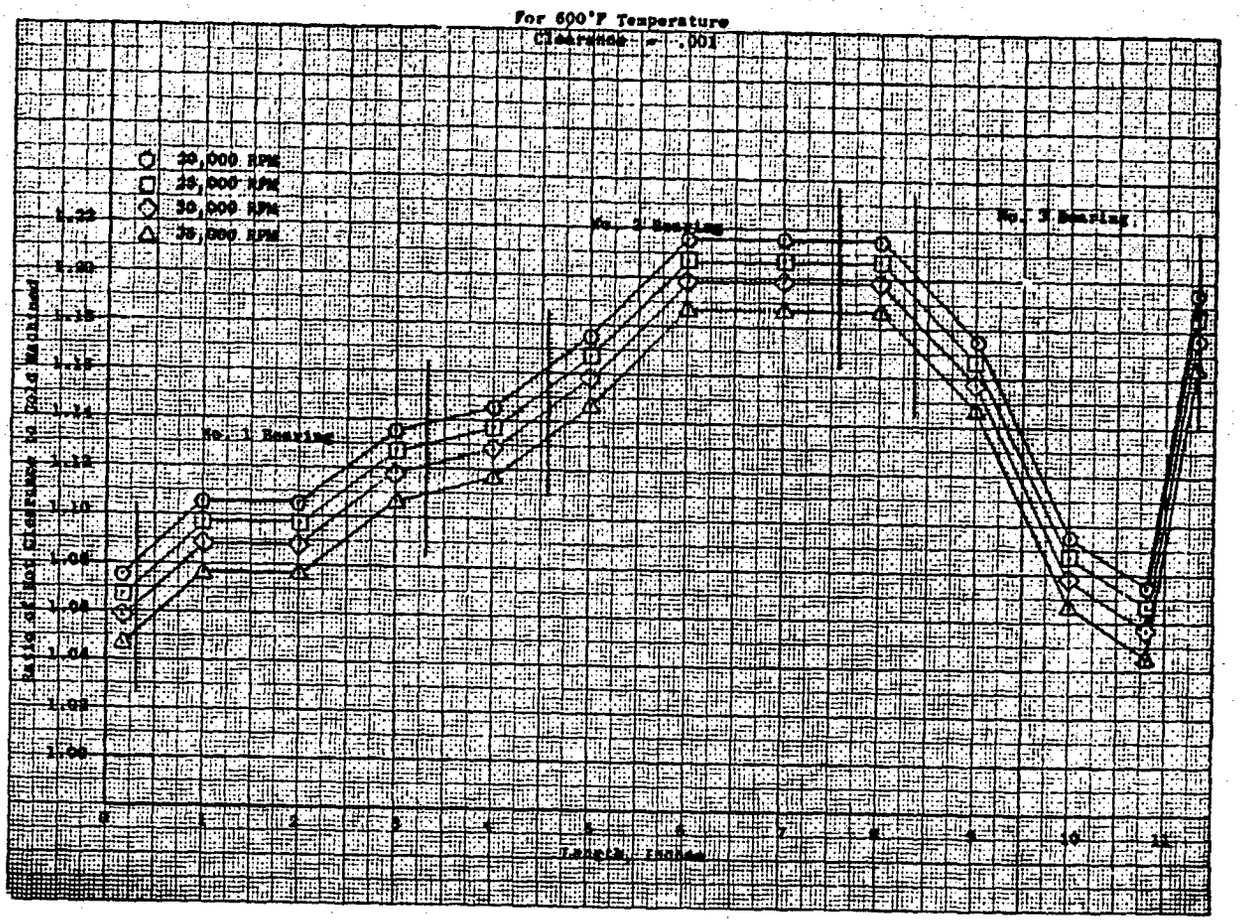

Figure 7. Bearing Clearance

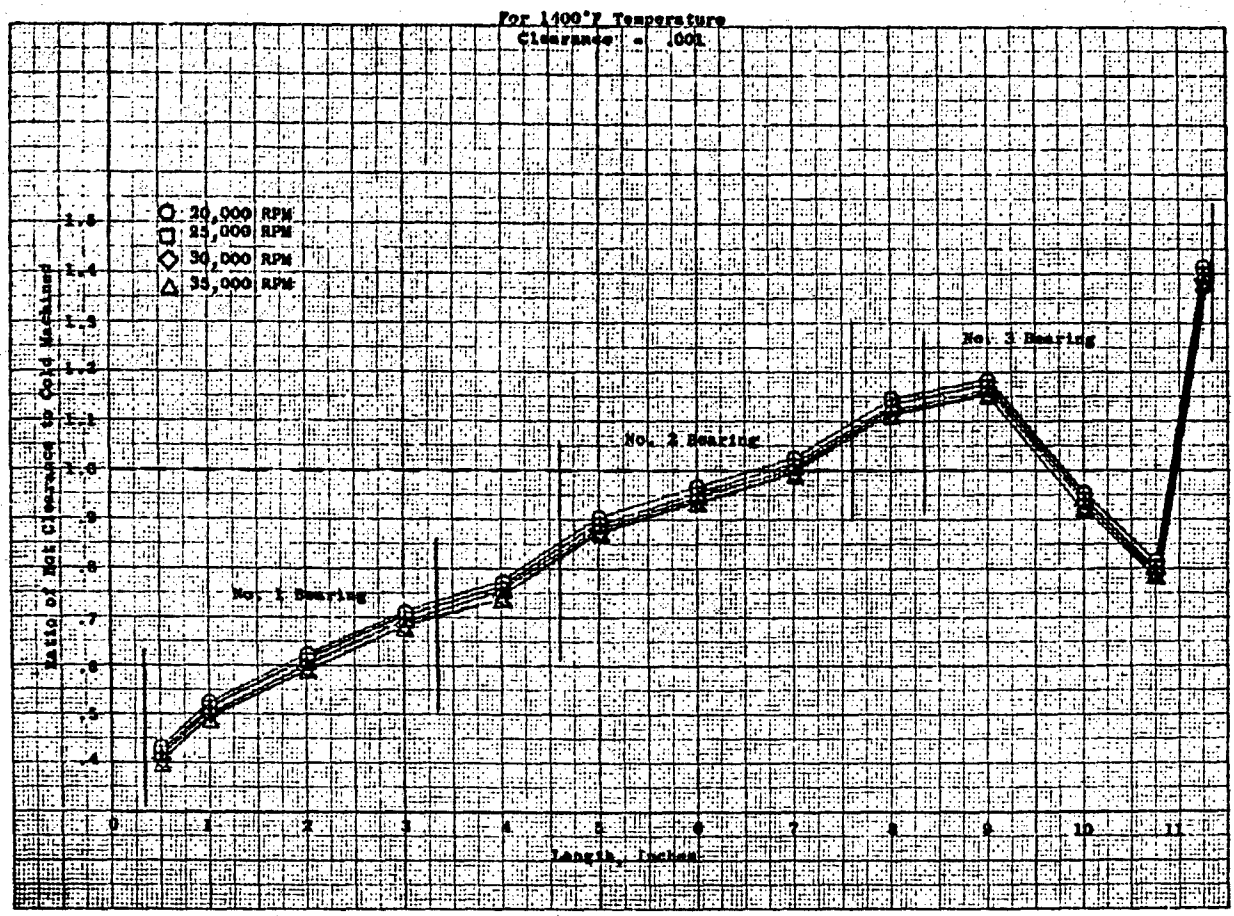

Figure 8. Bearing Clearance

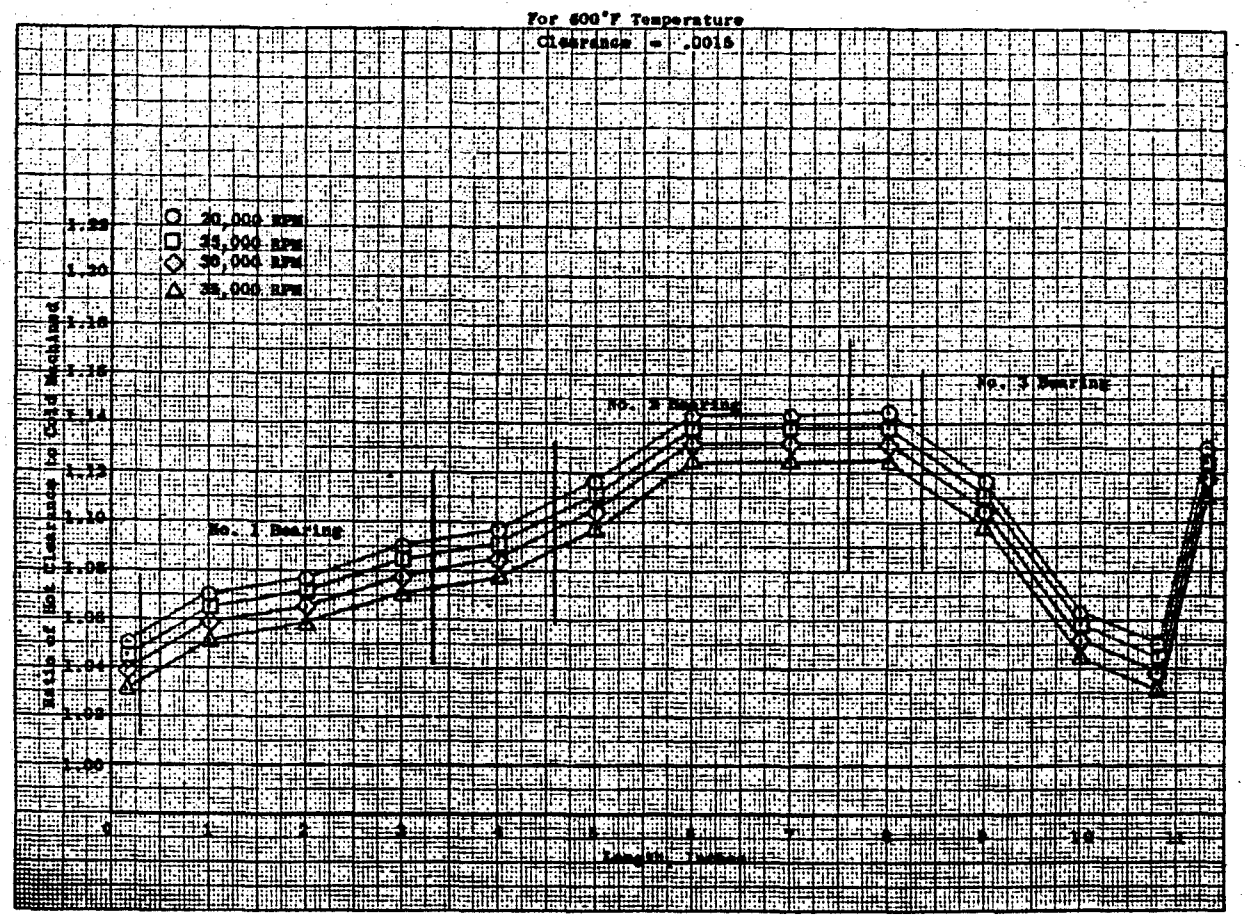

Figure 9. Bearing Clearance

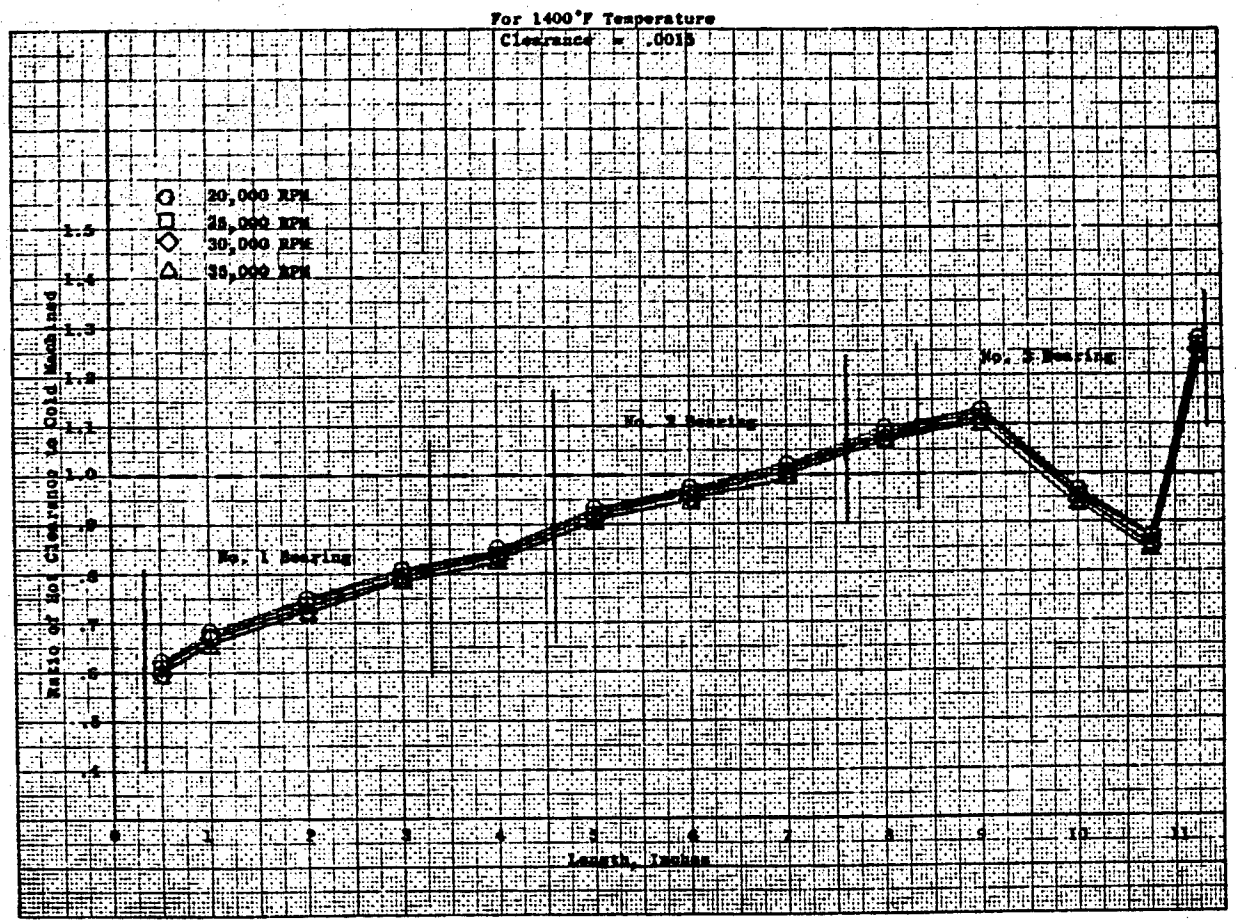

Figure 10. Bearing Clearance

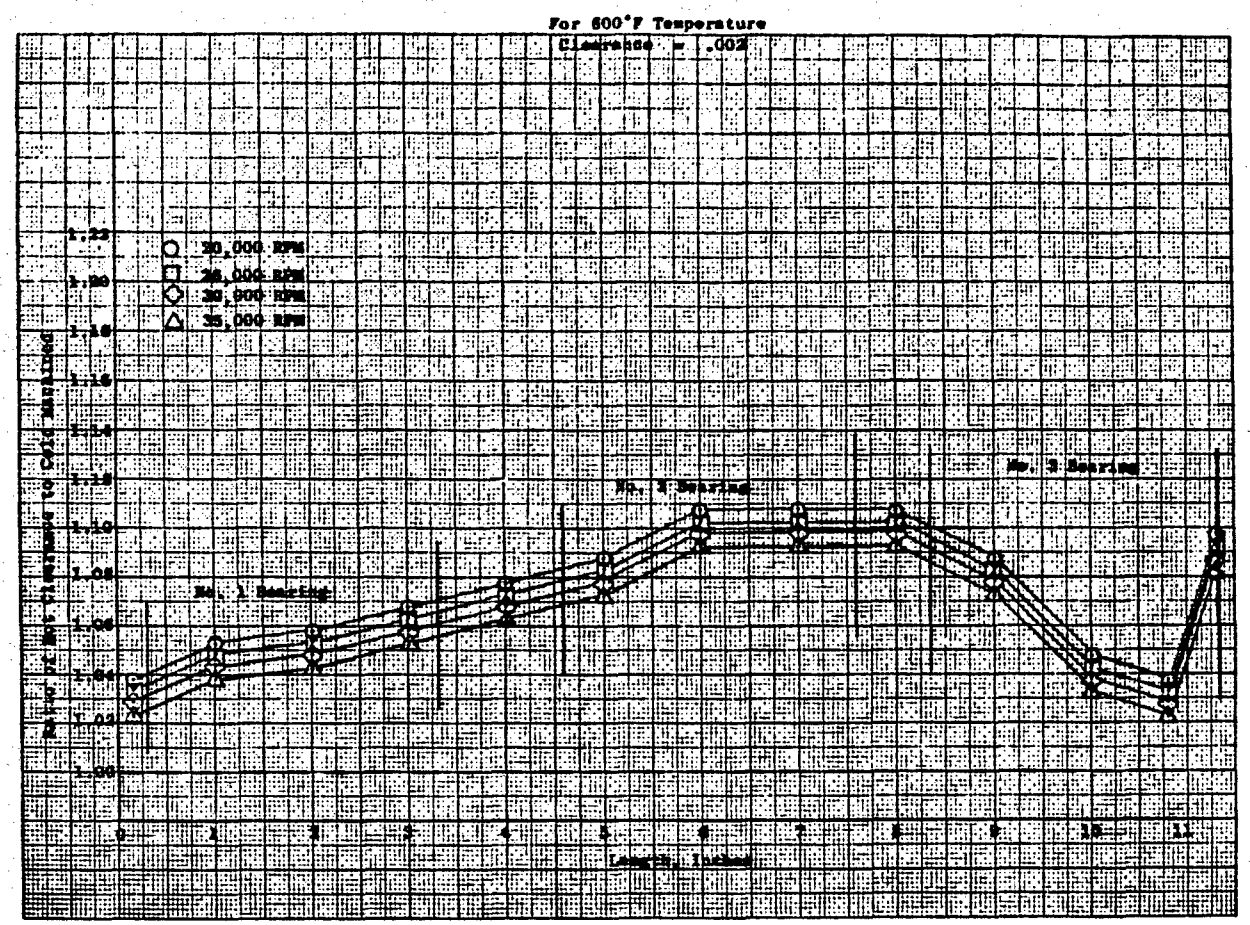

Figure 11. Bearing Clearance

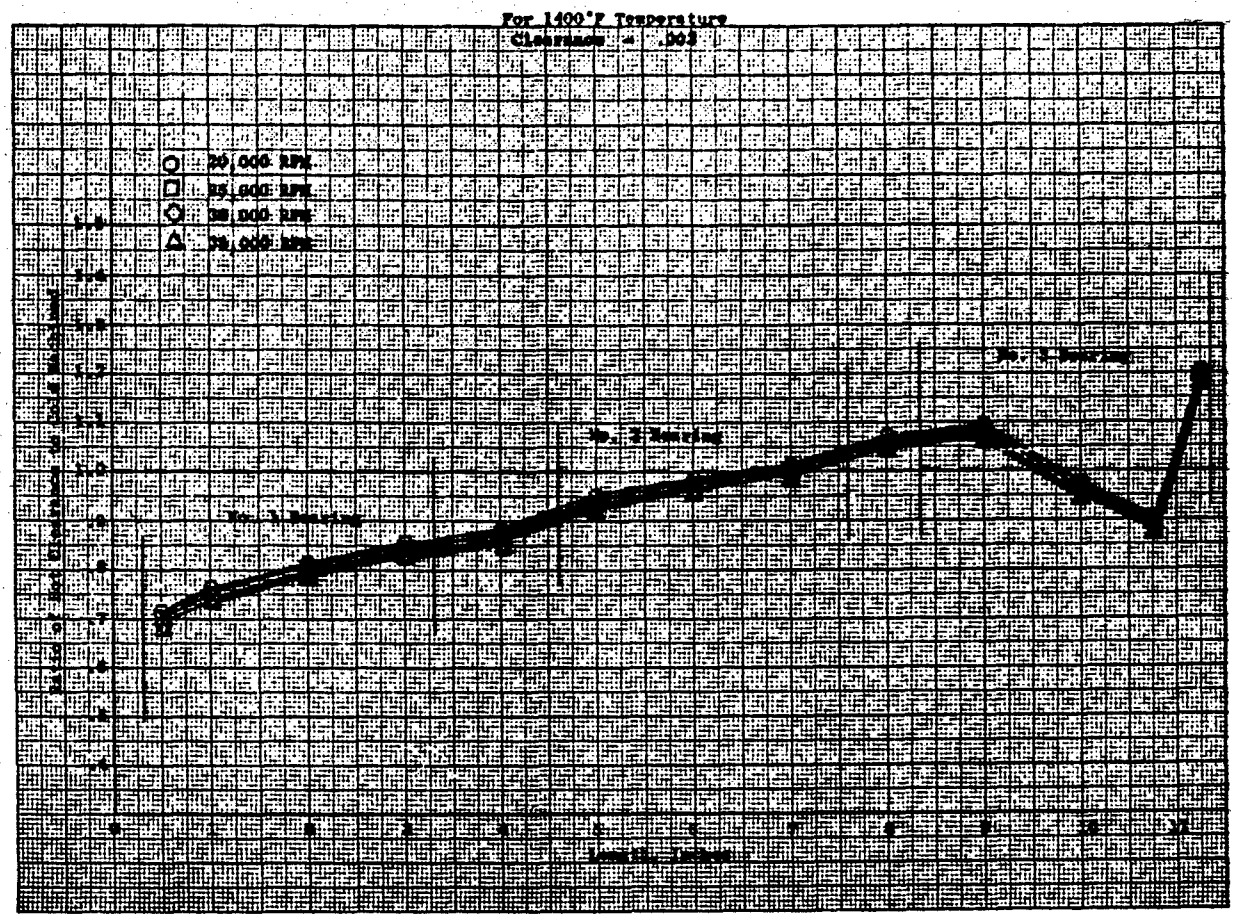

Figure 12. Bearing Clearance

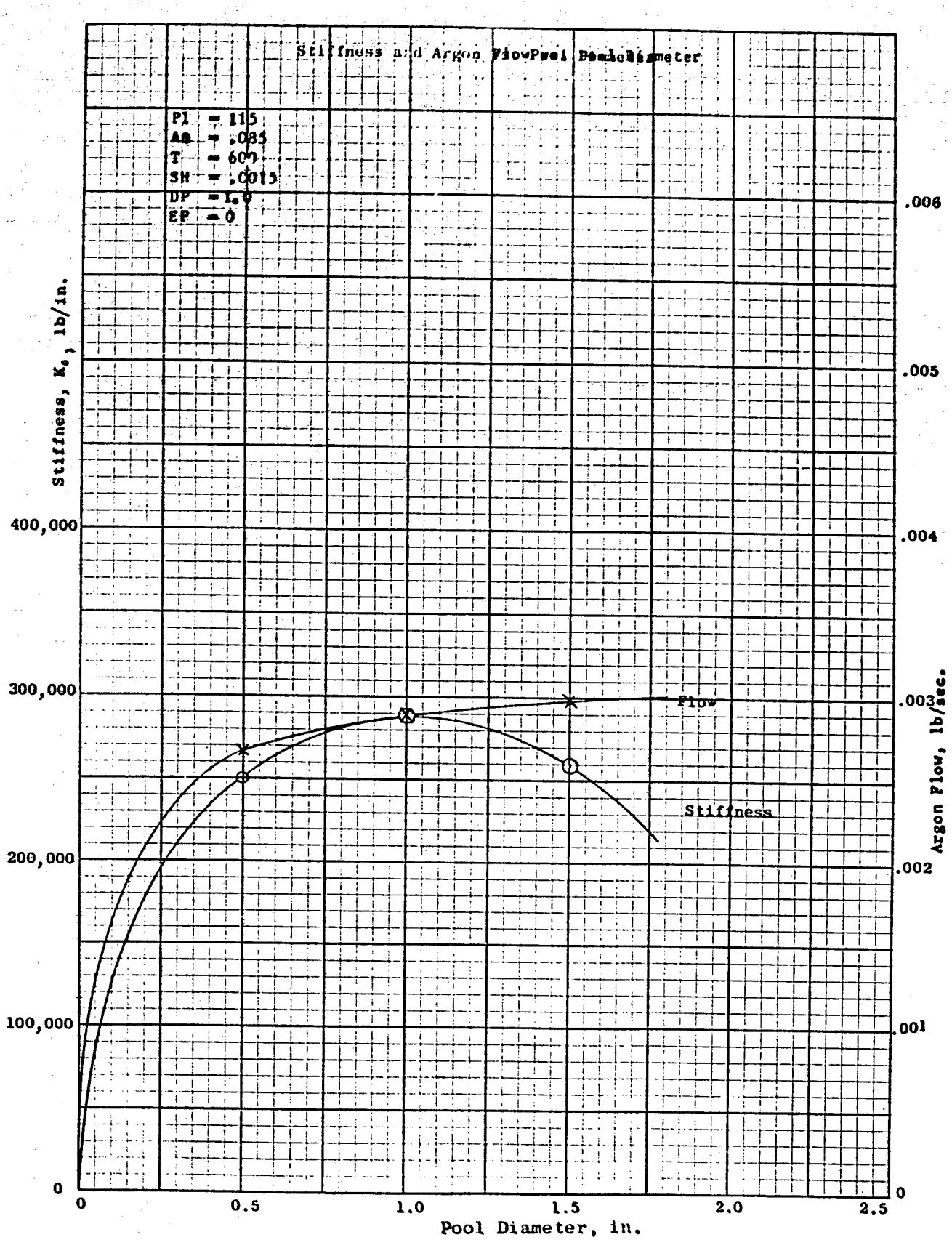

Figure 13. Stiffness and Flow vs. Pool Diameter

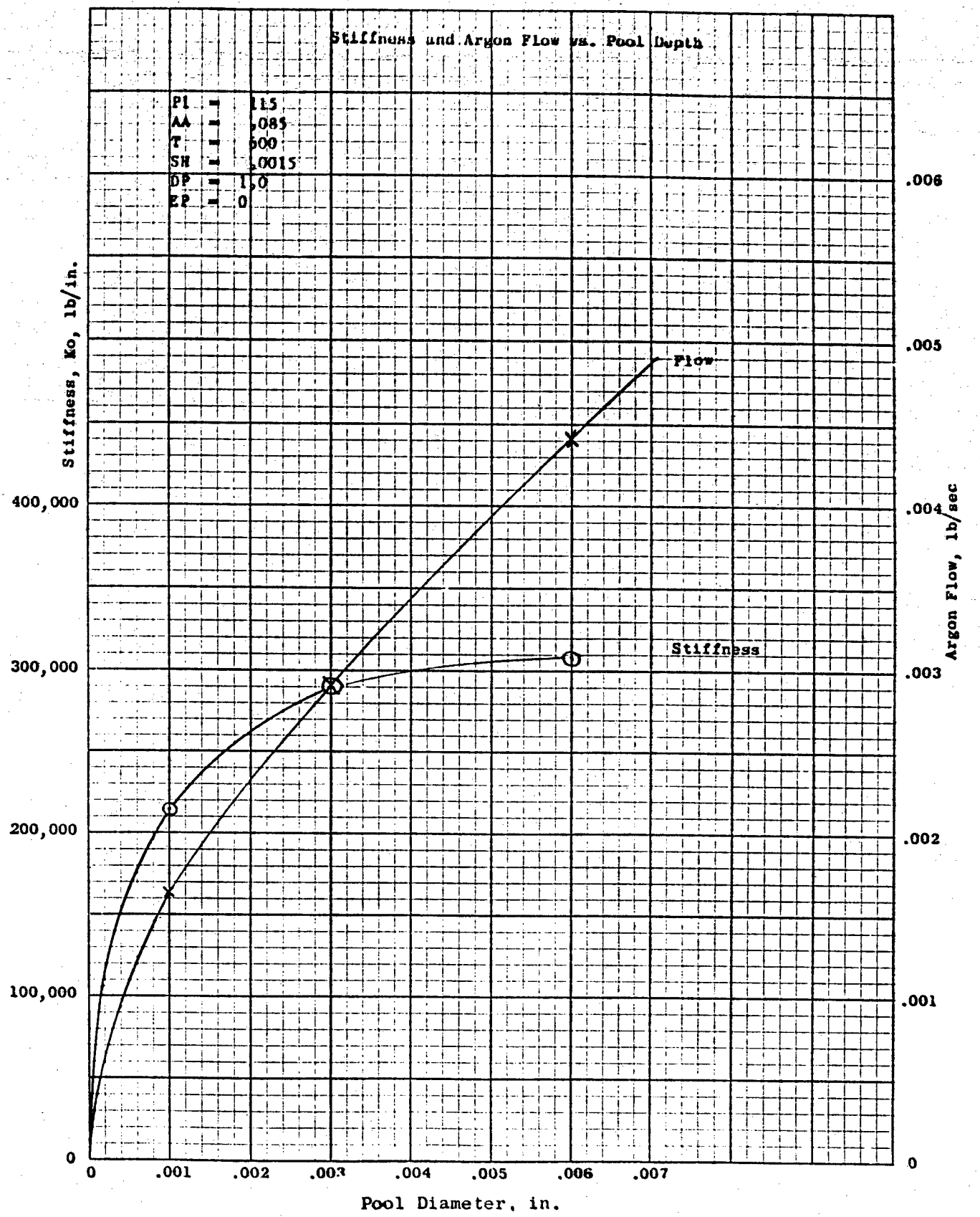

Figure 14. Stiffness and Flow vs. Pool Depth

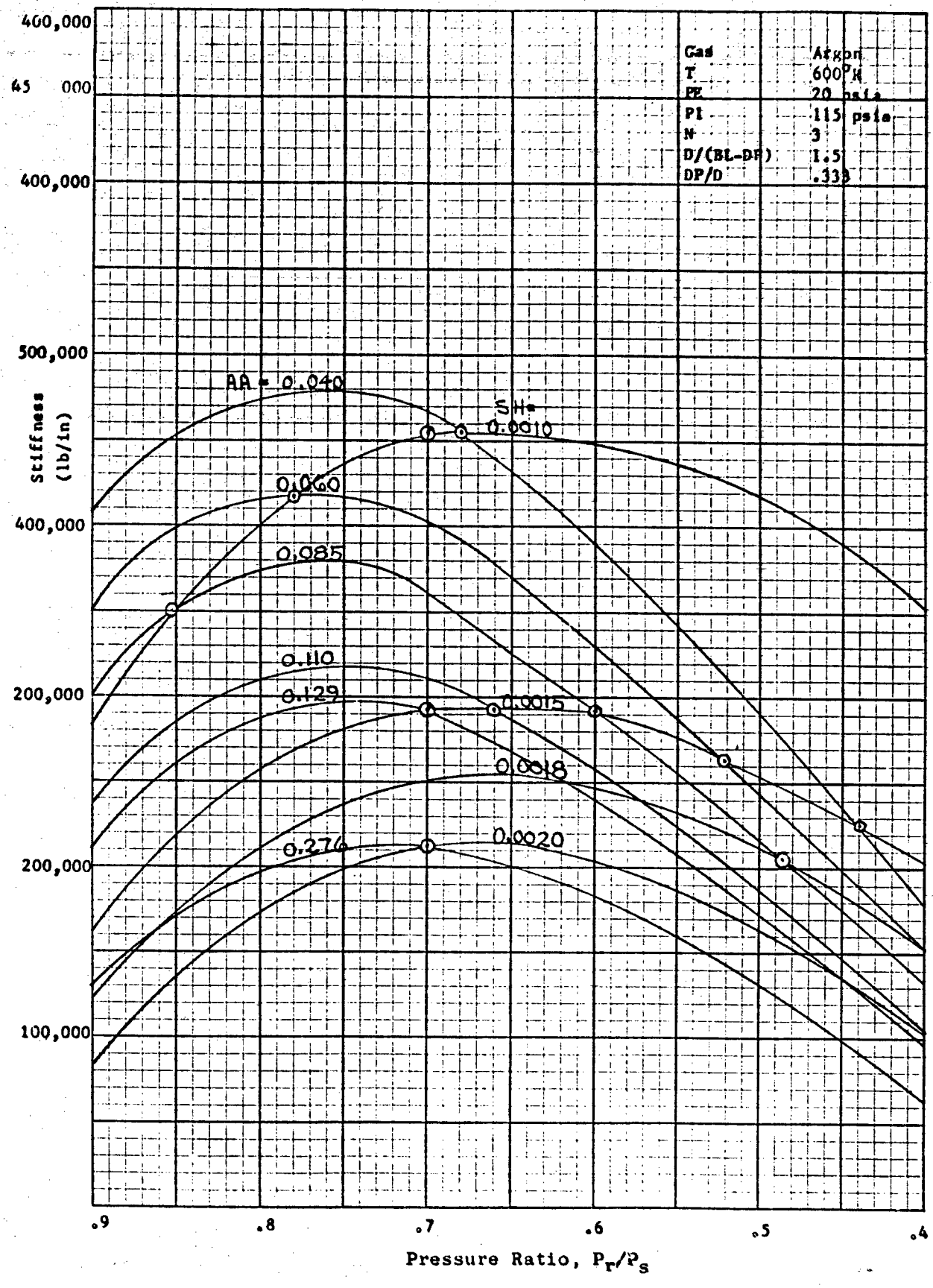

Figure 15. Stiffness vs. Pressure Ratio

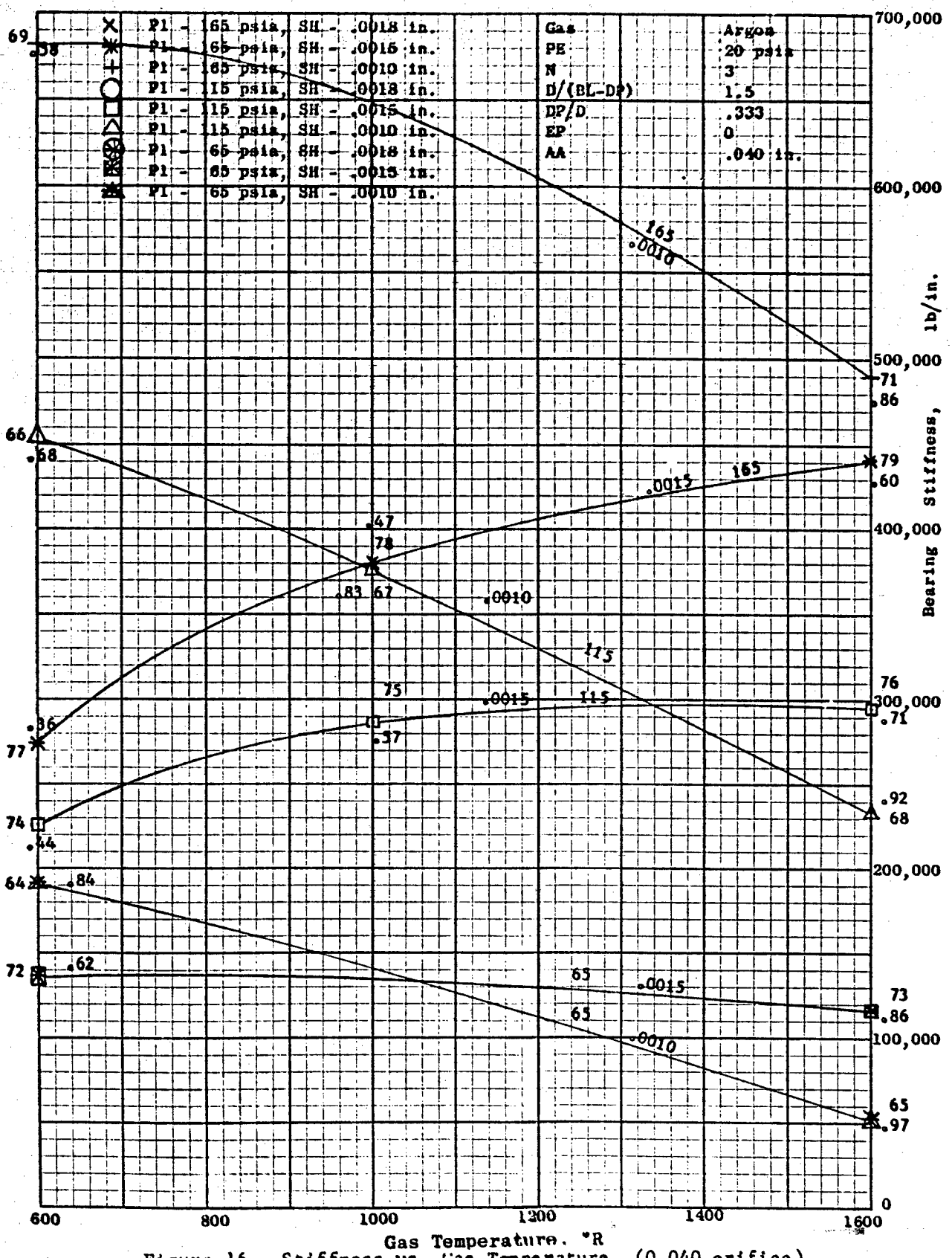

Figure 16. Stiffness vs. Gas Temperature, (0.040 orifice)

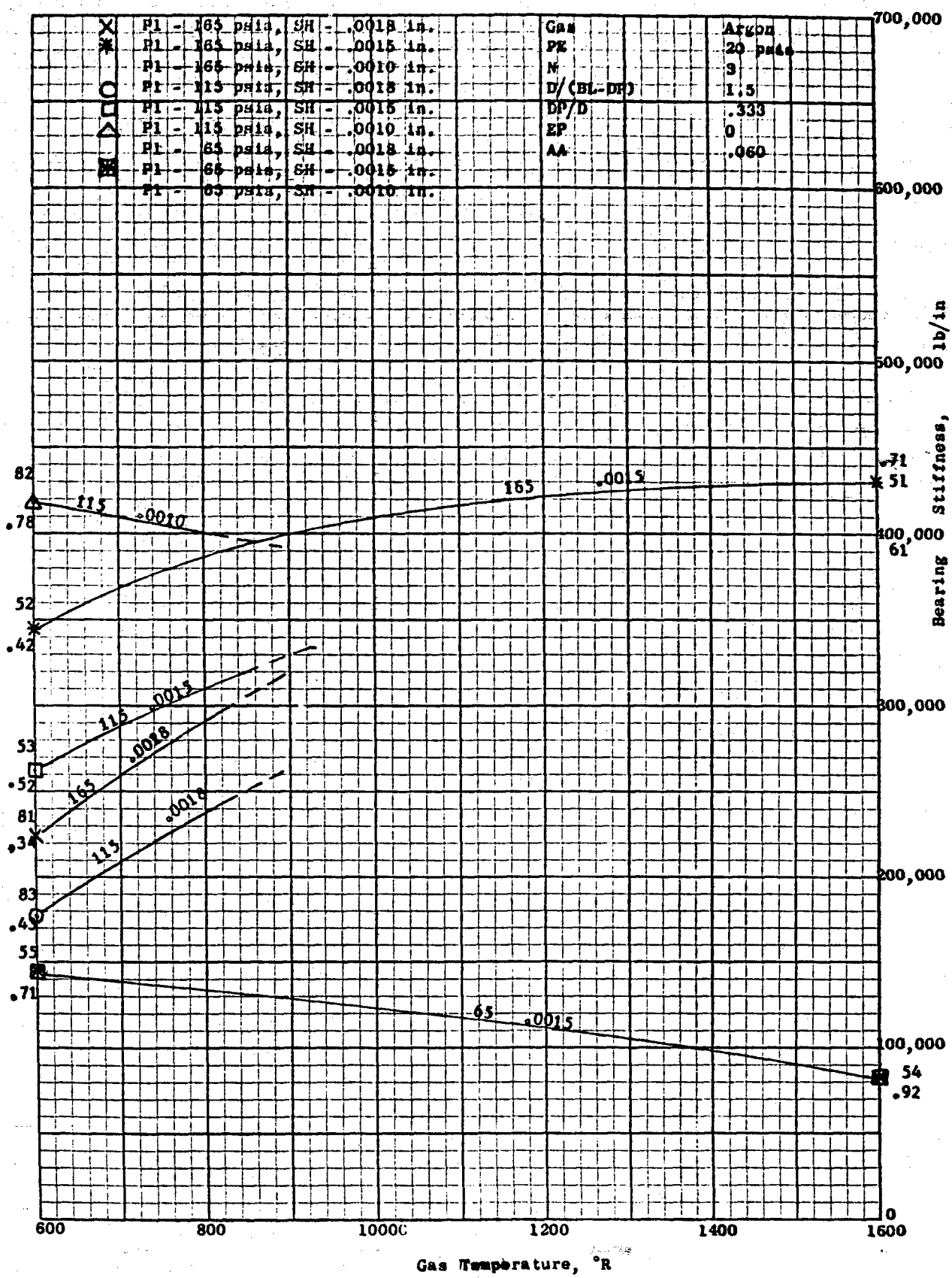

Figure 17. Stiffness vs. Gas Temperature, (0.060 orifice)

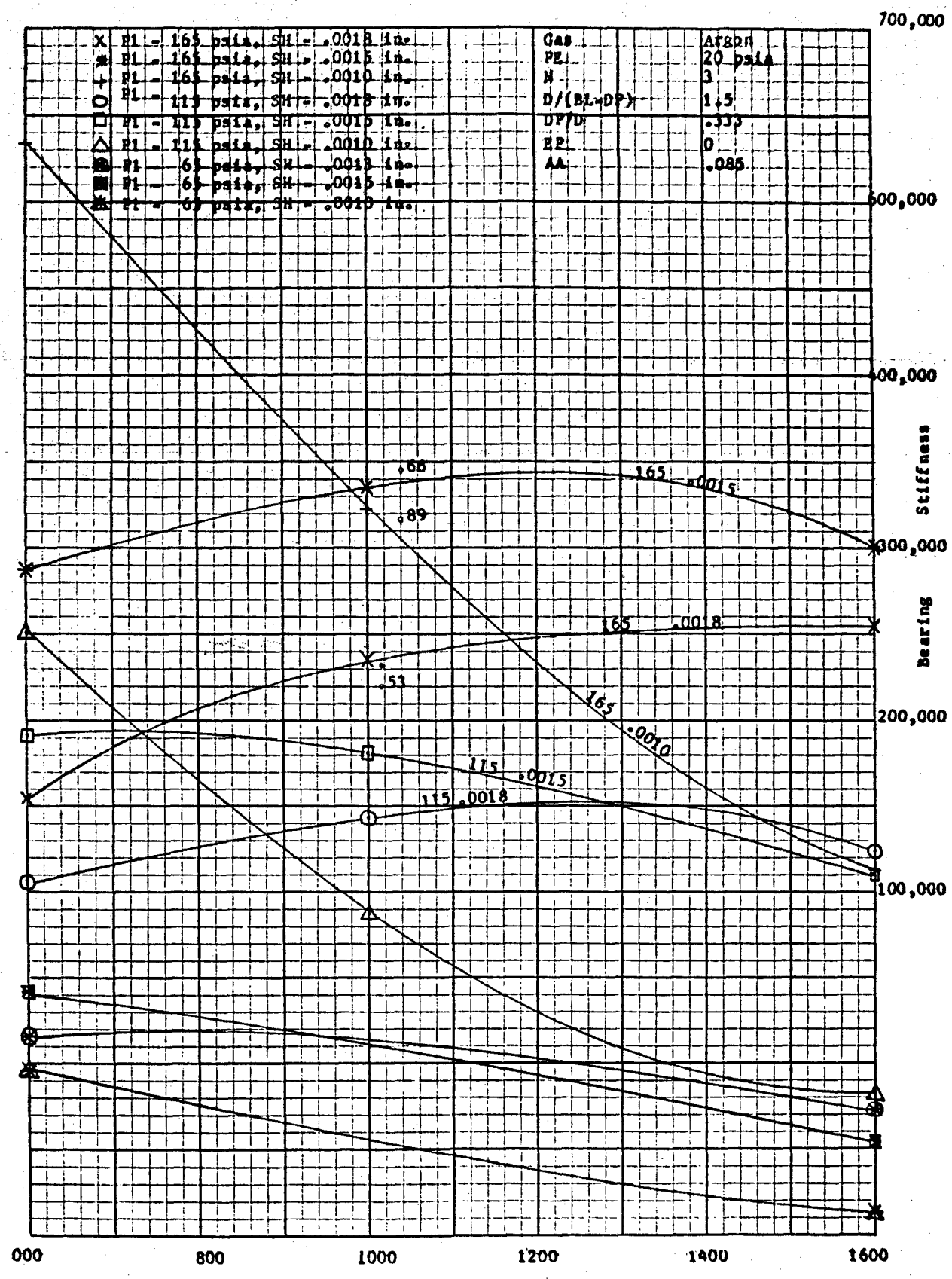

Figure 18. Stiffness vs. Gas Temperature, (0.085 orifice)

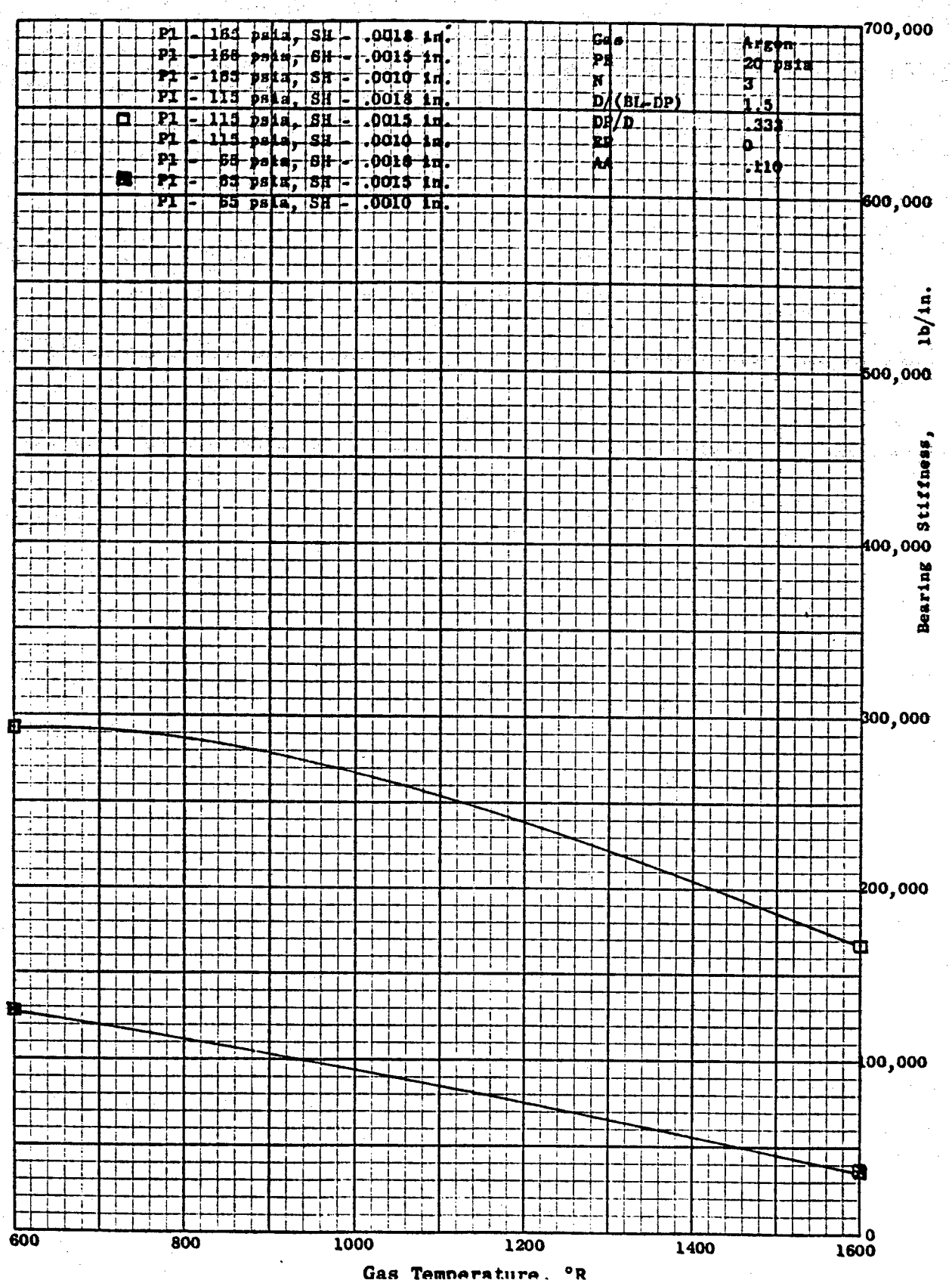

Figure 19. Stiffness vs. Gas Temperature, (0.110 orifice)

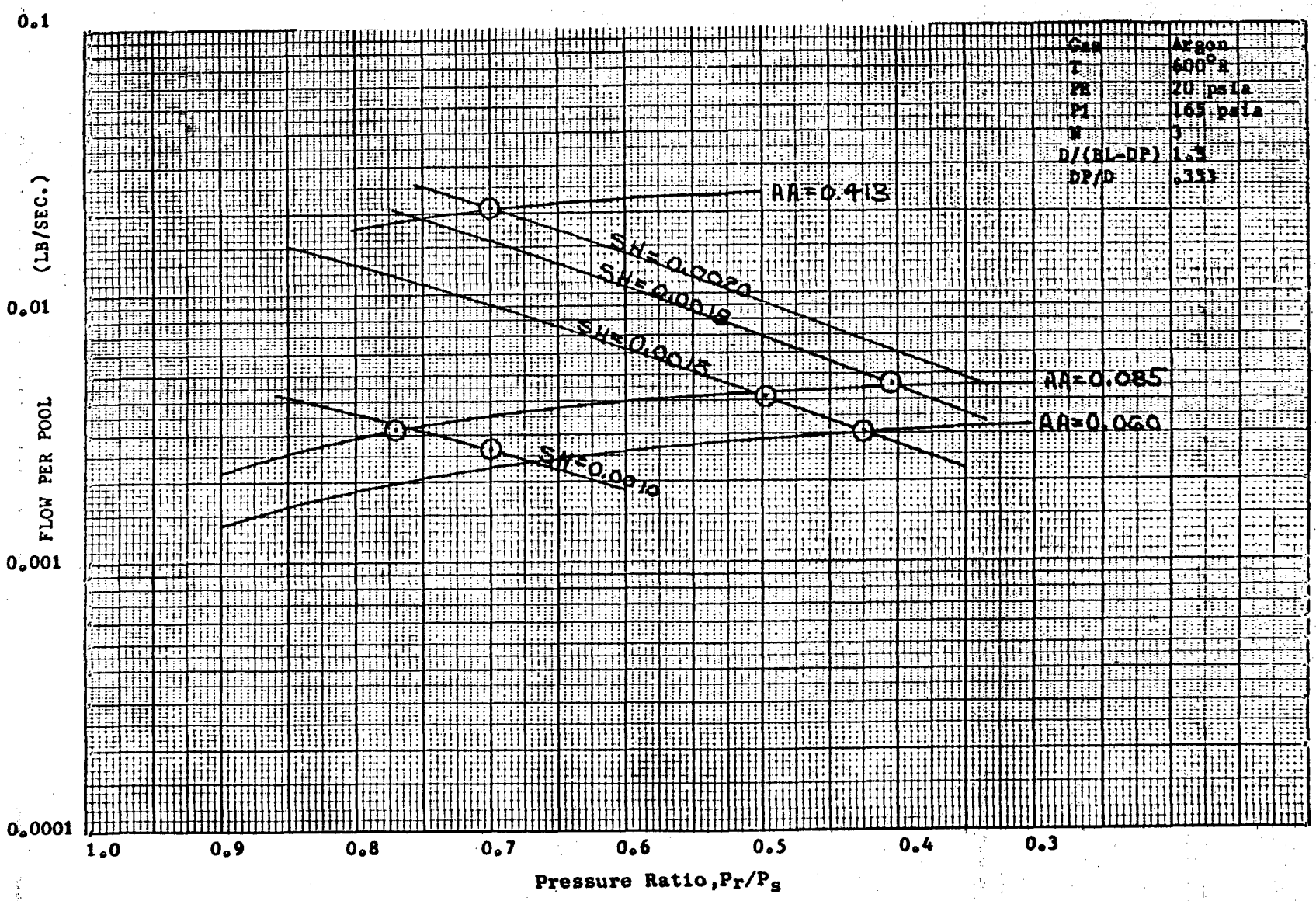

Figure 20. Flow vs. Pressure Ratio, (165 psia, 600°R)

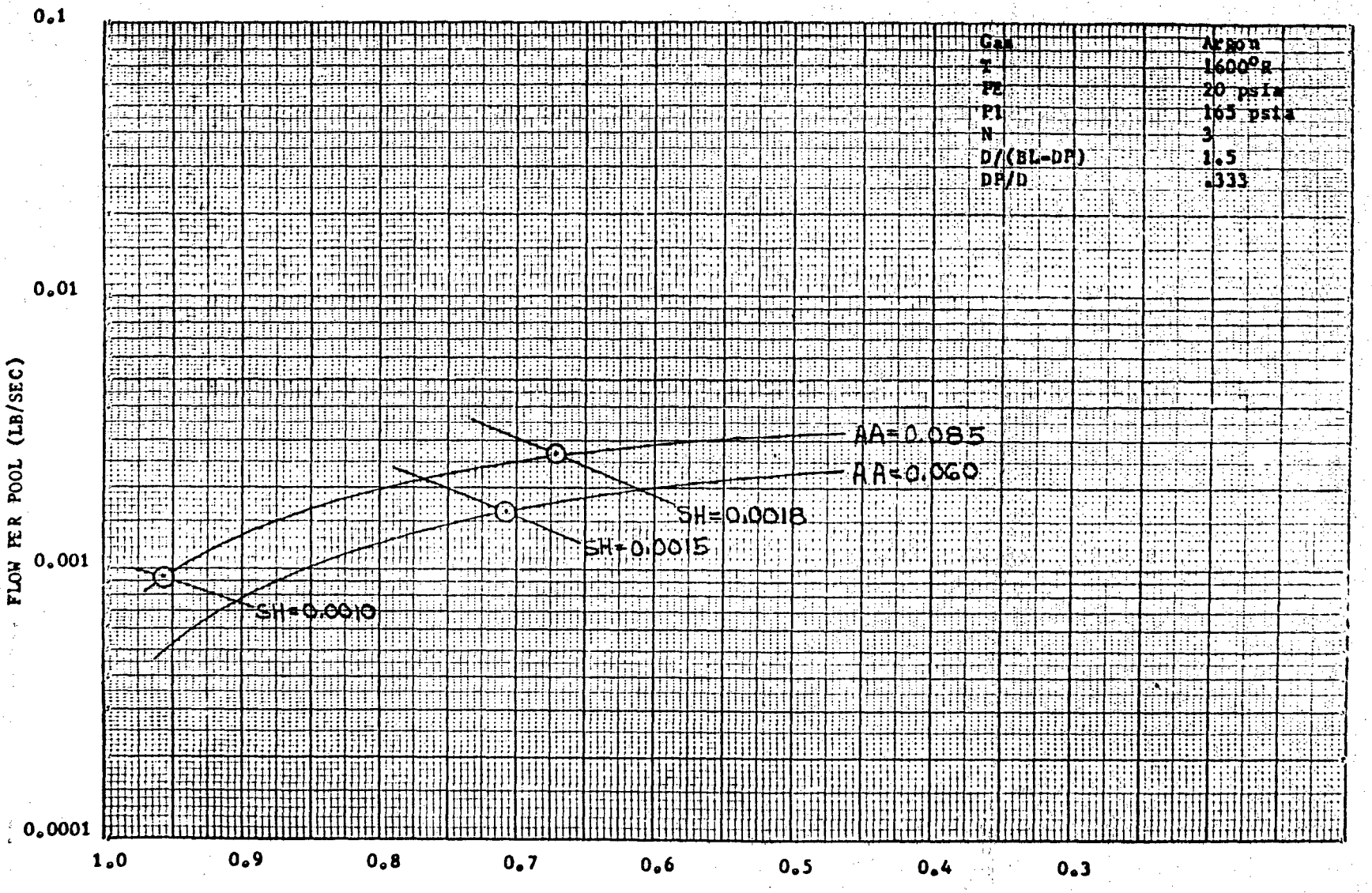

Figure 21. Flow vs. Pressure Ratio, (165 psia, 1600°R)

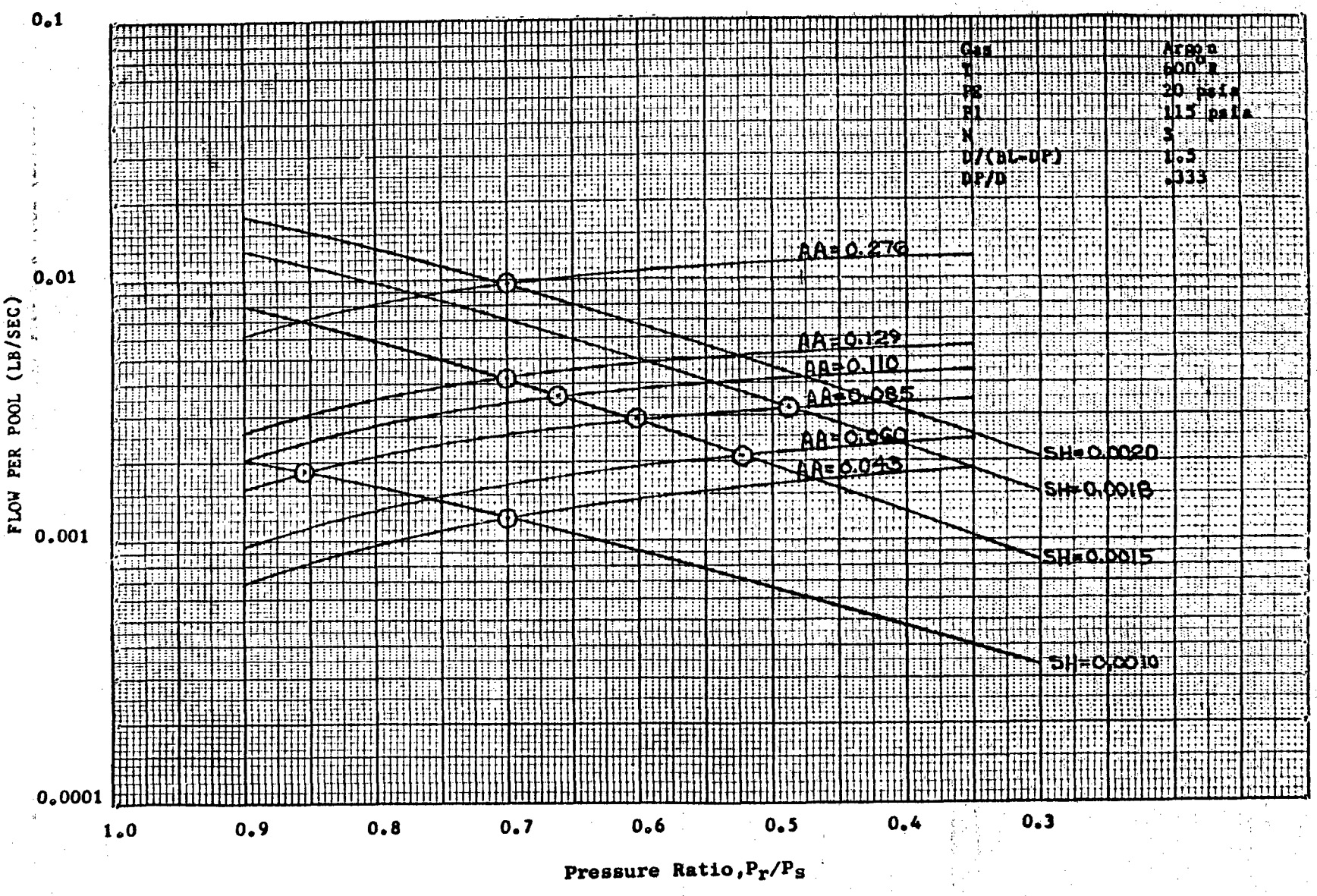

Figure 22. Flow vs. Pressure Ratio, (115 psia, 600°R)

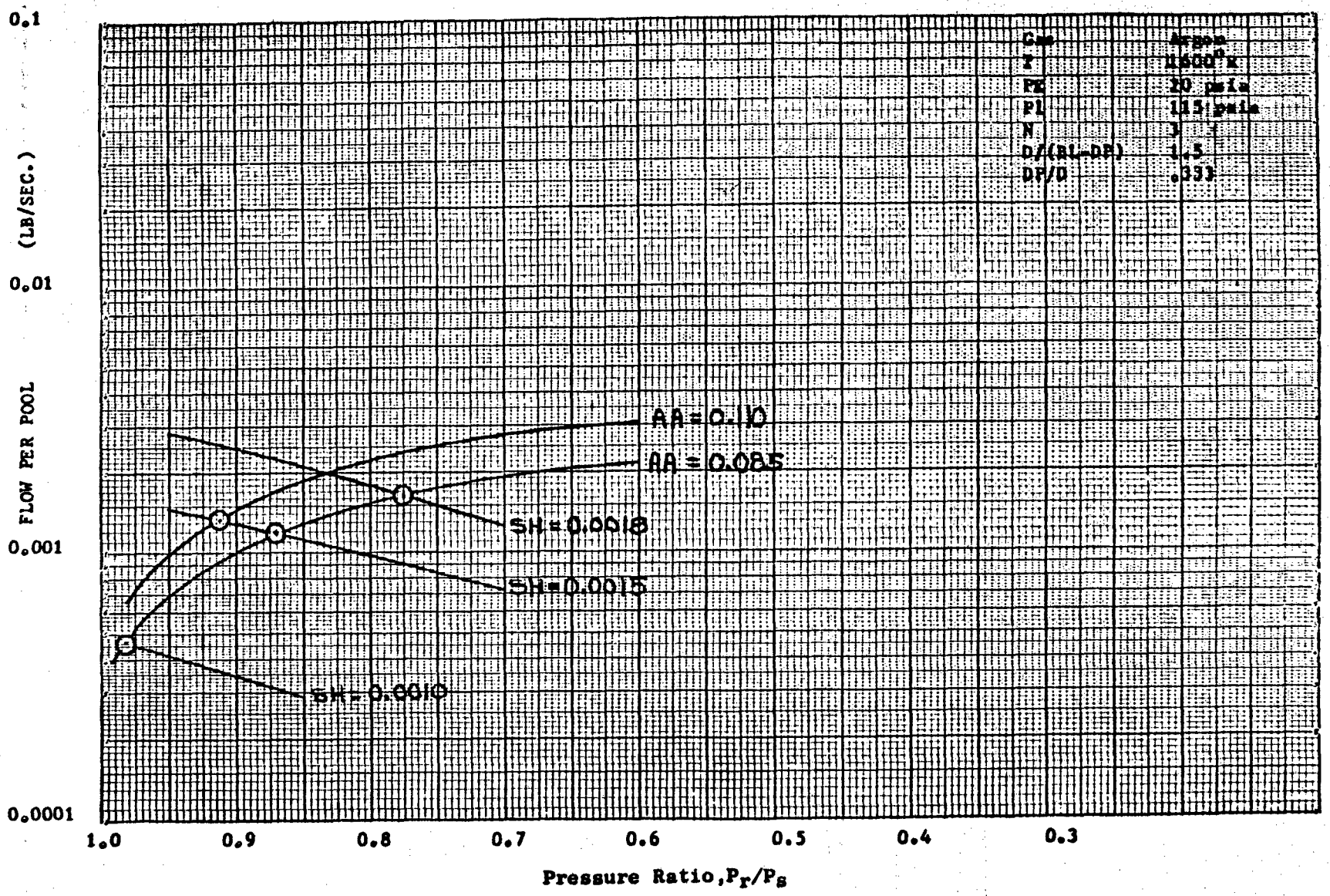

Figure 23. Flow vs. Pressure Ratio, (115 psia, 1600°R)

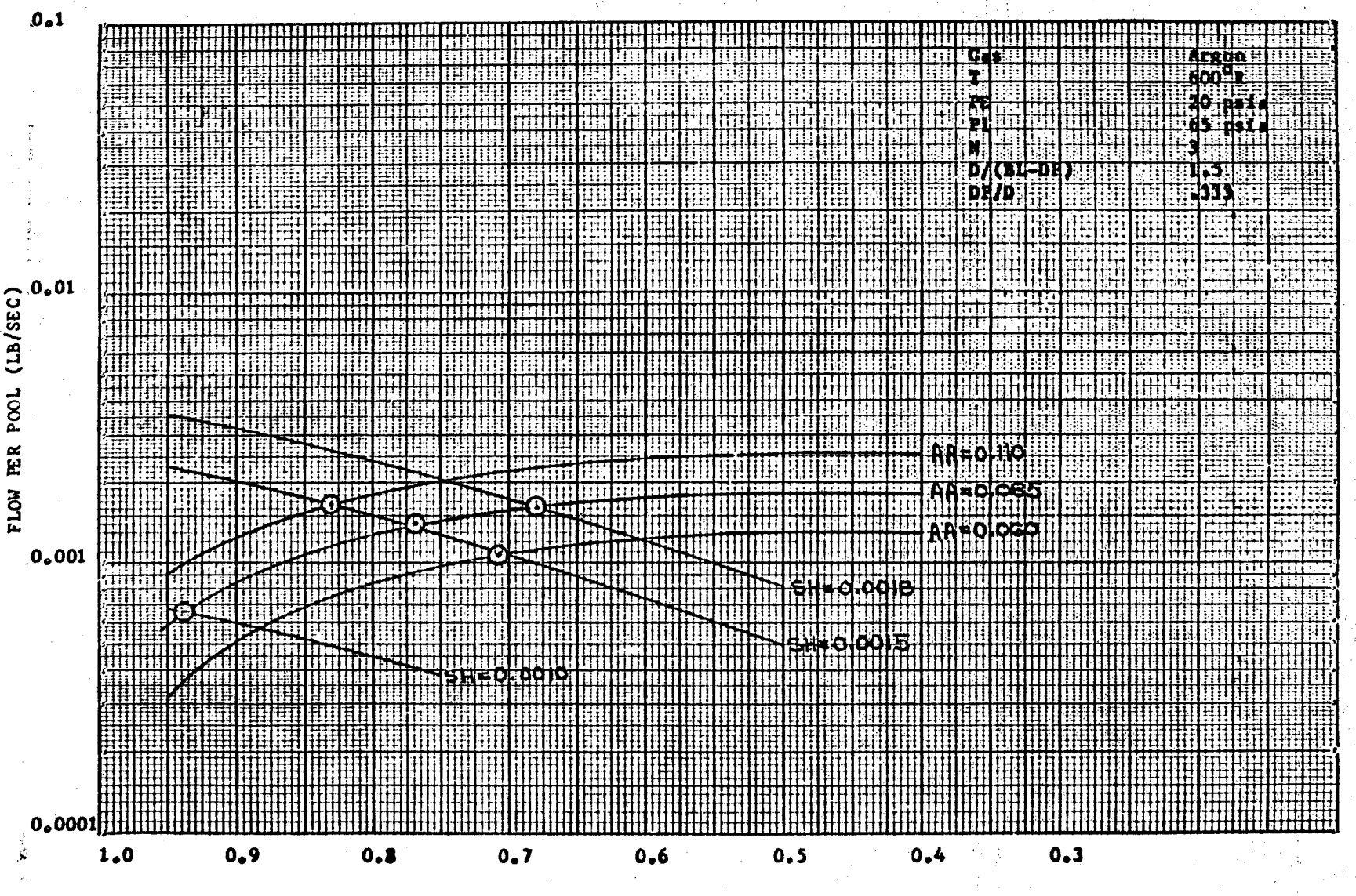

Figure 24. Flow vs. Pressure Ratio, (65 psia, 600°R)

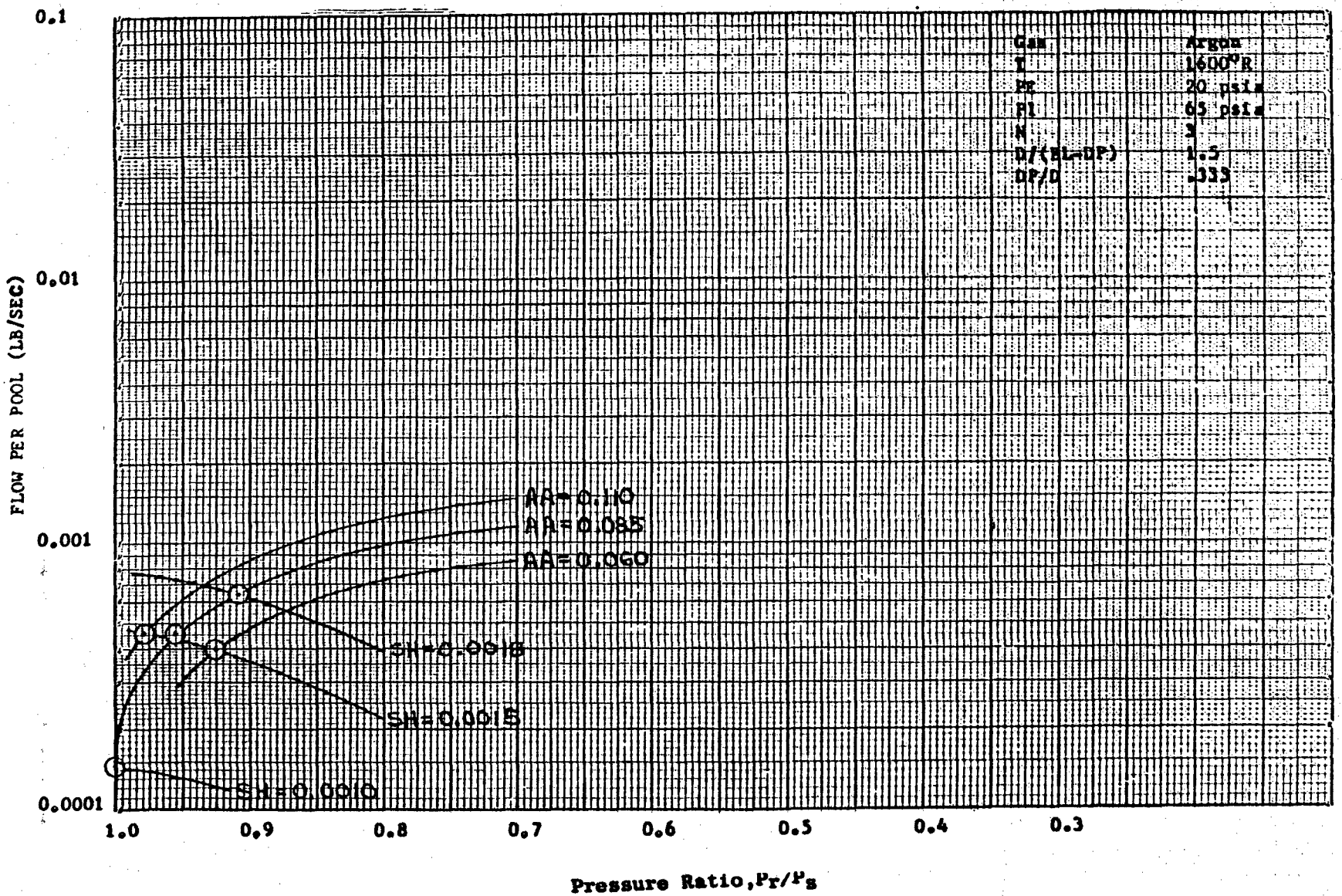

Figure 25. Flow vs. Pressure Ratio, (65 psia, 1600°R)

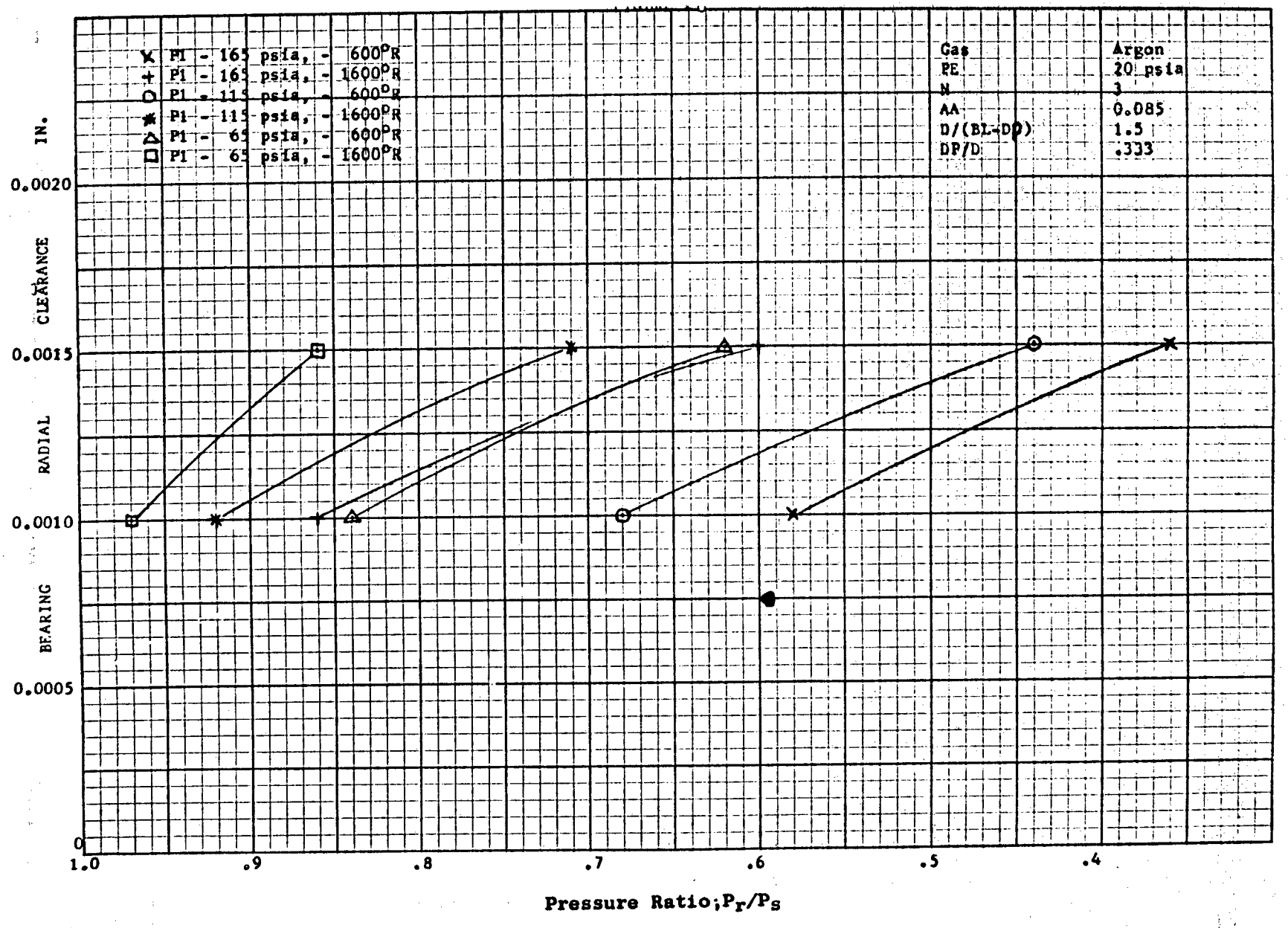

Figure 26. Radial Clearance vs. Pressure Ratio, (0.040 orifice)

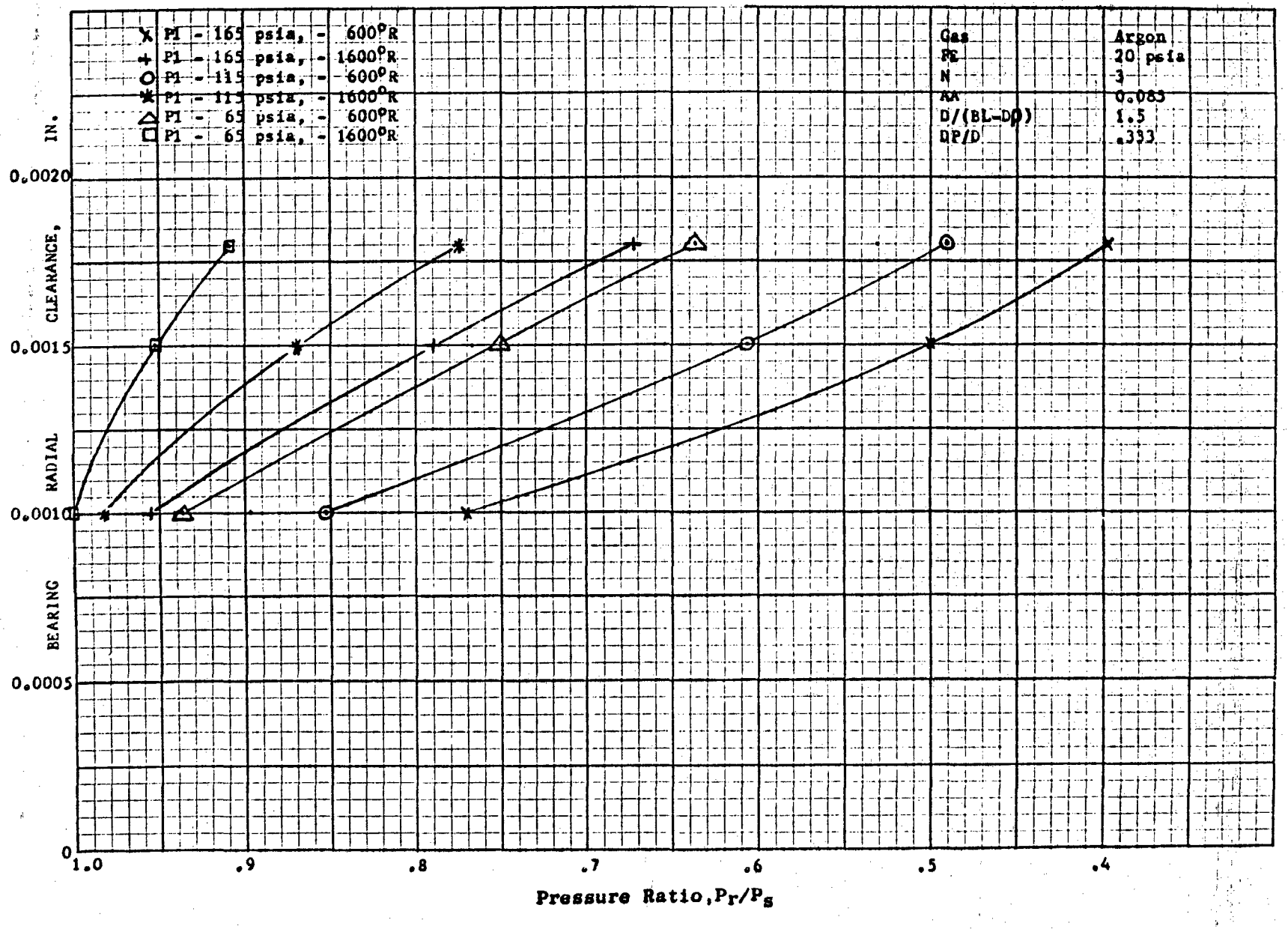

Figure 27. Radial Clearance vs. Pressure Ratio, (0.085 orifice)

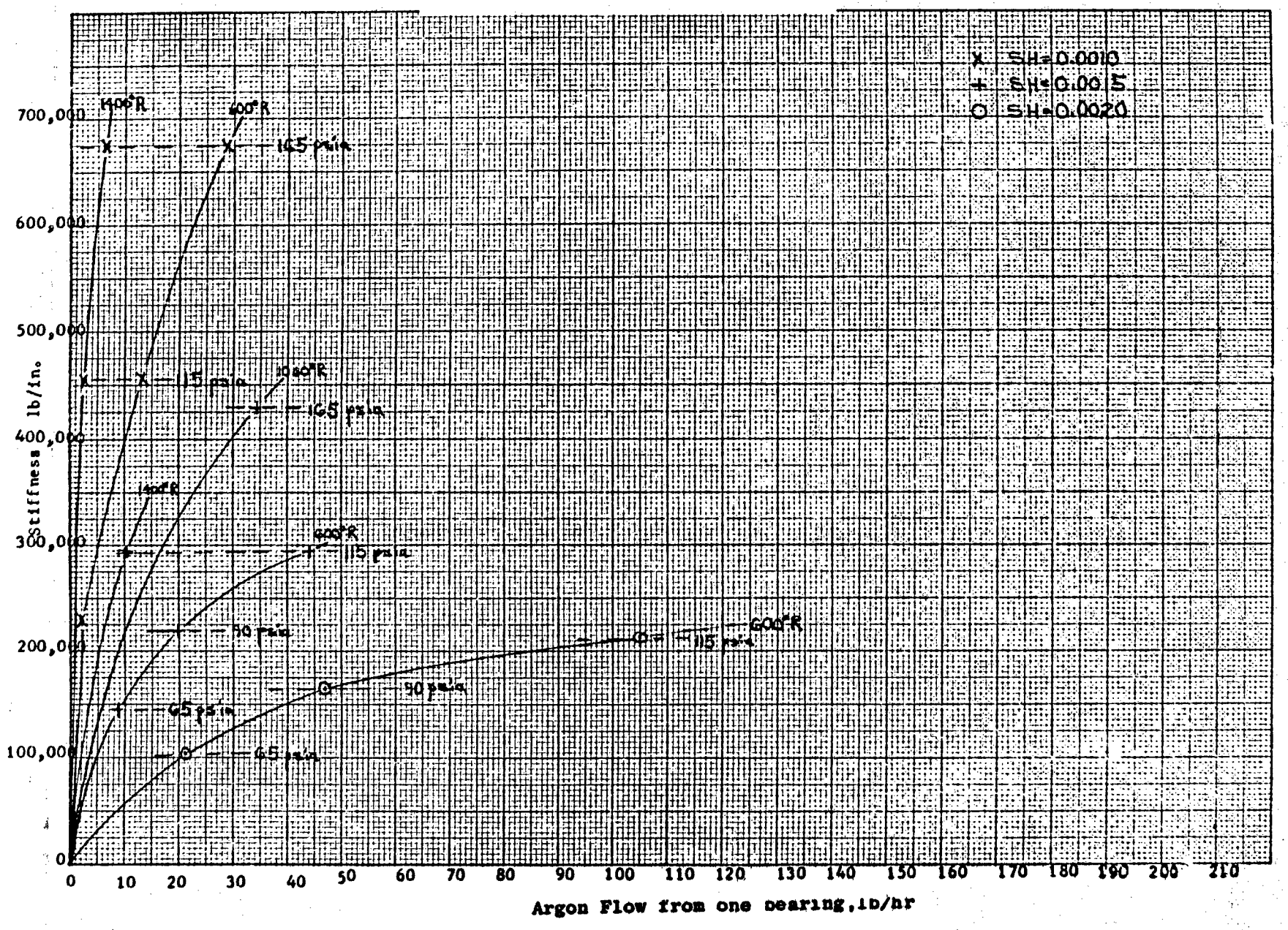

Figure 28. Stiffness vs. Flow, (SH=0.0015, PR=0.7)

DISTRIBUTION LIST

Copies	Organization
1	ASD (ASRCNL-2, Mr. John Morris) Wright Patterson AFB, Ohio
1	ASD (ASNPFS-3, Mr. R. Ling) Wright Patterson AFB, Ohio
1	ASD (ASRCNL, Mr. G. A. Beane) Wright Patterson AFB, Ohio
2	ASD (ASRMFP-3, Mr. R. J. Smith) Wright Patterson AFB, Ohio
1	U. S. Atomic Energy Commission Office of Technical Information P. O. Box 62 Oak Ridge, Tennessee
1	Thompson Ramo Wooldridge Attn: Mr. Carl Nau 23555 Euclid Avenue Cleveland 17, Ohio
1	Rocketdyne Division North American Aviation Attn: Mr. R. B. Dillaway Department 584 6633 Canoga Park Boulevard Canoga Park, California
1	Technical Information Center Aerospace Corporation P. O. Box 95085 Los Angeles 45, California
10	ASTIA Arlington Hall Station Arlington 12, Virginia

1	Cleveland Graphite Bronze Division of Clevite Corporation Attn: Mr. E. James Vargo 17000 St. Clair Avenue Cleveland 10, Ohio
1	SSD (SSTRE, Capt. W. W. Hoover) AF Unit Post Office Los Angeles 45, California
1	Power Information Center Moore School Building 200 South 33rd Street Philadelphia 4, Pennsylvania
1	National Aeronautics and Space Administration Lewis Research Center Attn: Mr. Joseph Joyce Space Electric Power Office 25000 Brookpark Road Cleveland 35, Ohio
1	AiResearch Manufacturing Company Attn: Mr. John Dennan 402 - 536th Street Phoenix 34, Arizona
1	Sundstrand Aviation Corporation Attn: Mr. K. Nichols 2480 West 70 Denver 21, Colorado
1	Aerojet-General Nucleonics Attn: Mr. Paul Wood Azusa, California
1	Pratt & Whitney Aircraft Division of United Aircraft Corp. Attn: Mr. Frederick A. Corwin East Hartford, Connecticut

1	Mechanical Technology Inc., Attn: Mr. F. K. Orcutt Albany-Shaker Road Latham, New York
1	Ion Physics Corporation Attn: Dr. A. Stuart Denholm P. O. Box 98 Burlington, Mass.
1	Mr. G. G. Thur NASA-Lewis Research Center 21000 Brookpark Road Cleveland 35, Ohio